RESEARCH ARTICLE

Blockade or Deletion of IFNγ Reduces Macrophage Activation without Compromising CAR T-cell Function in Hematologic Malignancies

Stefanie R. Bailey[1,2], Sonika Vatsa[1], Rebecca C. Larson[1,2], Amanda A. Bouffard[1], Irene Scarfò[1,2], Michael C. Kann[1], Trisha R. Berger[1], Mark B. Leick[1,2,3], Marc Wehrli[1,2], Andrea Schmidts[1,2], Harrison Silva[1], Kevin A. Lindell[1], Ashley Demato[1], Kathleen M.E. Gallagher[1,4], Matthew J. Frigault[1,2,3], and Marcela V. Maus[1,2,3]

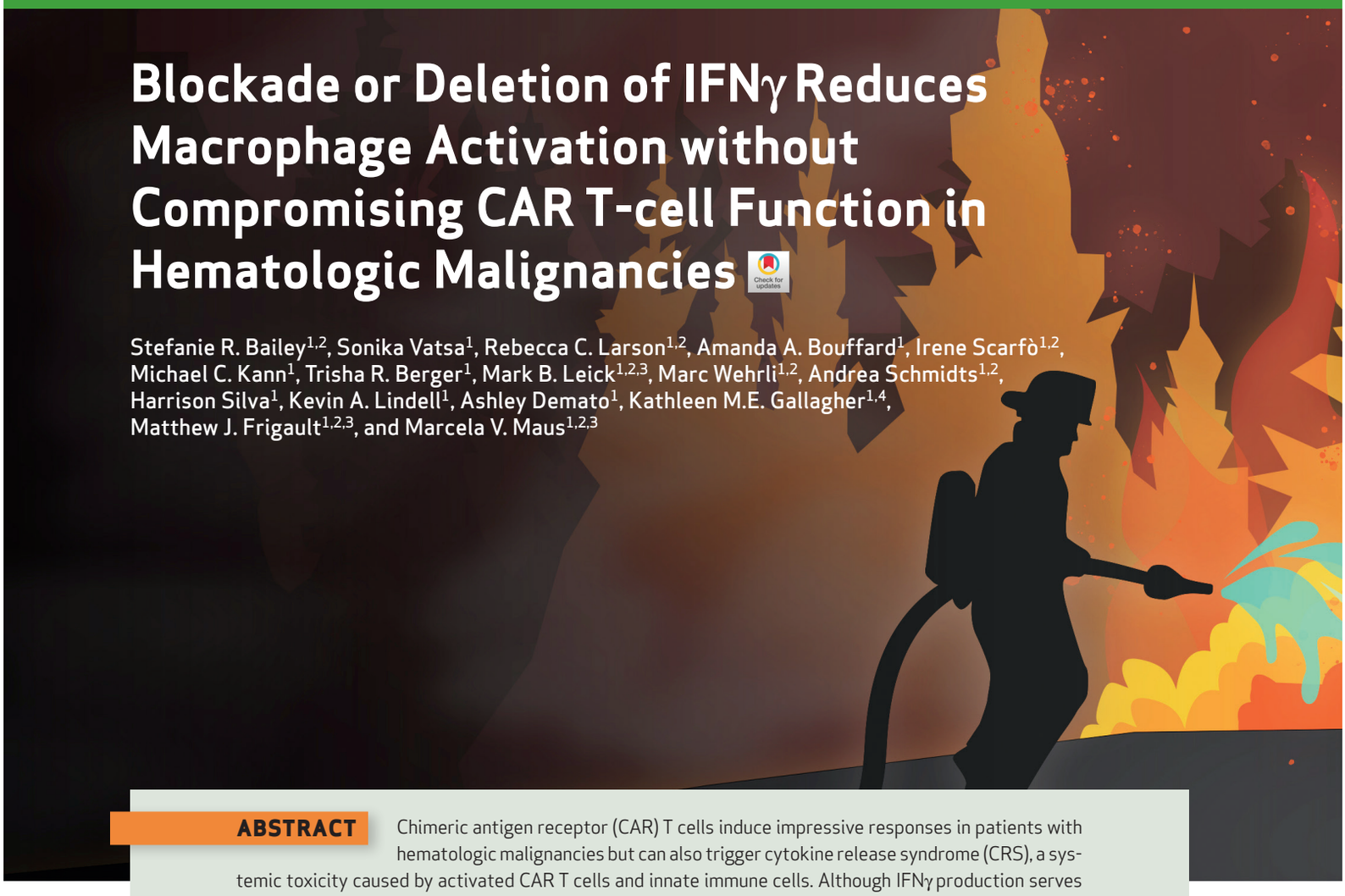

ABSTRACT Chimeric antigen receptor (CAR) T cells induce impressive responses in patients with hematologic malignancies but can also trigger cytokine release syndrome (CRS), a systemic toxicity caused by activated CAR T cells and innate immune cells. Although IFNγ production serves as a potency assay for CAR T cells, its biologic role in conferring responses in hematologic malignancies is not established. Here we show that pharmacologic blockade or genetic knockout of IFNγ reduced immune checkpoint protein expression with no detrimental effect on antitumor efficacy against hematologic malignancies *in vitro* or *in vivo*. Furthermore, IFNγ blockade reduced macrophage activation to a greater extent than currently used cytokine antagonists in immune cells from healthy donors and serum from patients with CAR T-cell–treated lymphoma who developed CRS. Collectively, these data show that IFNγ is not required for CAR T-cell efficacy against hematologic malignancies, and blocking IFNγ could simultaneously mitigate cytokine-related toxicities while preserving persistence and antitumor efficacy.

SIGNIFICANCE: Blocking IFNγ in CAR T cells does not impair their cytotoxicity against hematologic tumor cells and paradoxically enhances their proliferation and reduces macrophage-mediated cytokines and chemokines associated with CRS. These findings suggest that IFNγ blockade may improve CAR T-cell function while reducing treatment-related toxicity in hematologic malignancies.

See interview with Stefanie R. Bailey, PhD, recipient of the 2023 Blood Cancer Discovery Award for Outstanding Journal Article: https://vimeo.com/847433865

See related content by McNerney et al., p. 90 (17).

[1]Cellular Immunotherapy Program, Cancer Center, Massachusetts General Hospital, Boston, Massachusetts. [2]Department of Medicine, Harvard Medical School, Boston, Massachusetts. [3]Blood and Marrow Transplant Program, Massachusetts General Hospital, Boston, Massachusetts. [4]Department of Pathology, Harvard Medical School, Boston, Massachusetts.

Corresponding Author: Marcela V. Maus, 149 13th Street, Room 3.216, Charlestown, MA 02129. Phone: 617-724-3853; E-mail: mvmaus@mgh.harvard.edu

Blood Cancer Discov 2022;3:136–53

doi: 10.1158/2643-3230.BCD-21-0181

INTRODUCTION

IFNγ is a cytokine produced primarily by T cells and NK cells and plays an important role in orchestrating immune responses in cancer and infectious diseases. Specifically, IFNγ activates innate immune cells (macrophages; refs. 1, 2), and upregulates both antigen-presentation pathways and immune checkpoint proteins (3–6) in immune cells and tumor cells (7). Because IFNγ production is easily measured and reliably triggered following CAR T-cell engagement with antigen, measurements of IFNγ release have emerged as the *de facto* potency assay for CAR T-cell therapeutic products, despite the lack of a clear role for IFNγ in mediating their antitumor efficacy in hematologic malignancies. In melanoma and other solid tumors, mutations in IFNγ receptor signaling have been identified as a mechanism of resistance to checkpoint blockade (8, 9), and we have recently identified that IFNγ receptor signaling also confers relative resistance to CAR T-cell–mediated cytotoxicity only in solid tumors (10). In contrast, IFNγ produced by CAR T cells has a clear role in mediating cytokine release syndrome (CRS) and macrophage activation syndrome in hematologic malignancies. Patients suffering from CAR T-cell–associated toxicities, such as CRS and immune-effector cell–associated neurotoxicity syndrome (ICANS), have elevated levels of IFNγ (11–14), similar to patients with underlying rheumatologic or malignant disease that triggers macrophage activation syndrome, or genetic diseases that trigger hemophagocytic lymphohistiocytosis (HLH; refs. 12, 15, 16). Pharmacologic blockade of IFNγ using emapalumab-lzsg has recently been approved for the management of primary (genetic) HLH but has not yet been systematically tested with CAR T-cell–induced CRS or HLH, primarily due to concerns about potentially abrogating the antitumor effects; however, a recent case demonstrates that IFNγ antibody blockade may alleviate CRS without impacting antitumor efficacy (17).

We hypothesized that IFNγ is a by-product of CAR T-cell activation in hematologic malignancies that does not have direct antitumor effects but contributes to macrophage activation, which is associated with CAR T-cell toxicities. We sought to test this hypothesis using pharmacologic and genetic approaches to block or delete IFNγ in CAR T cells and probe the downstream effects in established and new models of both antitumor efficacy and toxicity,

respectively. These models leveraged both xenograft models of hematologic malignancies and serum samples derived from patients who went on to develop clinically significant cytokine-related toxicities.

RESULTS

IFNγ Blockade Does Not Affect CAR T-cell Subsets or Function

To define the role of IFNγ in CAR T-cell function, we leveraged pharmacologic and genetic approaches to block or delete IFNγ in cocultures of CD19-directed CAR T cells and CD19-positive leukemia and lymphoma tumor cells. Primary human T cells derived from healthy donors were transduced with a lentiviral vector encoding a CD19-specific CAR bearing a 4-1BB costimulatory domain (BBζ; Fig. 1A–C; Supplementary Fig. S1A). Following CAR T-cell expansion, IFNγ was successfully and specifically targeted with a blocking antibody (αIFNγ) in a dose-dependent manner (Fig. 1D; Supplementary Fig. S1B). Antibody-mediated blockade of IFNγ inhibited downstream signaling in the presence of recombinant human IFNγ, as demonstrated by reduced phospho-STAT1 (pSTAT1), and maintained stable expression of IFNγ receptor 1 (IFNγR1) on the surface of CAR T cells (Fig. 1E) and tumor cells, including JeKo-1 (mantle cell lymphoma; Fig. 1F), Nalm6 (acute lymphoblastic leukemia) and Raji (Burkitt lymphoma; Supplementary Fig. S1C and S1D). As expected, IFNγ blockade alone did not affect the expression of IFNγR1 or the viability of untransduced T cells (UTD), CAR T cells, or B-cell tumors (Supplementary Fig. S1E–S1H). On the basis of these data, we chose to move forward with two doses of IFNγ-blocking antibody offering moderate (5 μg/mL; ~60%) or high (20 μg/mL; ~90%) blockade of IFNγ signaling.

To genetically knock out IFNγ in CAR T cells, four IFNγ-targeted guides and a control GFP guide were purchased from the Broad Institute (Cambridge, MA) and assessed for their ability to knock out IFNγ in the T-cell line SMZ-1 (Supplementary Fig. S2A–S2C). The two guides that deleted IFNγ production in SMZ-1 cells compared with UTD and the GFP control were incorporated into CAR constructs, but one of these was more efficient at deleting IFNγ in primary CAR T cells while maintaining production of other cytokines; therefore, this guide was chosen for further studies (Supplementary Fig. S2D). To generate IFNγ knockout (KO) CAR T cells, healthy donor T cells were isolated, activated, and transduced with a lentiviral vector encoding the same CAR construct with the additional modification of upstream CRISPR/Cas9 guide RNA sequences for either the T-cell receptor α alone (TRAC KO) or in combination with the guide for IFNγ (IFNγKO; Fig. 1G–I; Supplementary Fig. S2E). Following Cas9 mRNA electroporation, KO and IFNγKO CAR T cells were isolated by removing $CD3^+$ T cells from the culture (Supplementary Fig. S2F), and specific deletion of IFNγ production in $CD3^-$ CAR T cells was confirmed by ELISA (Fig. 1J) and flow cytometry (Supplementary Fig. S2G and S2H). The deletion of IFNγ did not significantly alter the subsets of CAR T cells, as the two groups had similar ratios of CD4/CD8 T cells (Fig. 1K), with the majority being naïve ($CD62L^+CD45RO^-$) and expressing type 1 ($CXCR3^+CCR4^-CCR6^-$) or type 2 ($CCR4^+CCR6^-$) chemokine receptors (Supplementary Fig. S2I and S2J). There were no significant differences in memory subsets seen in $CD4^+$ or $CD8^+$ T cells. Like antibody blockade, IFNγKO CAR T cells did not alter expression of IFNγR1 on the cell surface or compromise viability following T-cell activation (Supplementary Fig. S2K and S2L).

Transcriptional analysis of KO CAR T cells following antigen stimulation through the CAR revealed strong donor-specific grouping with a weaker clustering among the KO and IFNγKO cells by principal component analyses (Supplementary Fig. S2M and S2N; Supplementary NanoString sequencing data file). As expected, *IFNG* expression was significantly reduced in IFNγKO CAR T cells compared with KO (Supplementary Fig. S2O). Collectively, these data demonstrate that IFNγ can be effectively blocked in CAR T cells by both pharmacologic and genetic approaches without significantly altering CAR T-cell subsets, viability, or transcriptional profiles.

IFNγ Is Not Required for Effective CAR T-cell Therapy in $CD19^+$ Hematologic Malignancies

We next sought to determine how the loss of IFNγ would affect CAR T-cell lysis of tumor cells *in vitro* and *in vivo*. ELISA confirmed that while IFNγ was decreased, protein levels of cytotoxic granules, such as granzyme B, were not different in antibody-blocked CAR T cells in response to antigen stimulation with $CD19^+$ cancer cells (Fig. 2A). Luciferase-based assays revealed that CAR T cells lysed JeKo-1, Nalm6, and Raji tumor cells in the presence of IFNγ blockade (5 and 20 μg/mL; Fig. 2B). Collectively, blocking IFNγ through antibody blockade had no effect on CAR T-cell cytotoxicity against CD19-expressing tumor cells *in vitro*.

To determine whether IFNγ was required for CAR T-cell antitumor efficacy *in vivo*, JeKo-1 lymphoma cells were intravenously injected into NSG mice 7 days prior to treatment with CD19-directed BBζ CAR T cells in combination with intraperitoneal injections of αIFNγ-blocking antibody or control IgG antibody (Fig. 2C). To evaluate the efficacy of the antibody blockade *in vivo*, serum was collected, and it was confirmed that IFNγ was reduced in mice receiving αIFNγ blockade (Fig. 2D). All mice receiving BBζ CAR T cells, regardless of IFNγ blockade, efficiently cleared the lymphoma (Fig. 2E and F). Further assessment revealed a similar CAR T-cell engraftment level in the blood and comparable overall survival of all treated mice (Fig. 2G and H). A similar protocol was followed using NSG mice bearing the more aggressive Nalm6 leukemia cells and confirmed that antibody blockade of IFNγ did not impact CAR T-cell persistence or efficacy *in vivo* (Fig. 2I–N). Interestingly, Nalm6-bearing mice that received anti-IFNγ–blocking antibody displayed significantly greater survival compared with mice that received BBζ + IgG or BBζ alone.

We next sought to determine how the genetic deletion of IFNγ affected CAR T-cell therapy of $CD19^+$ malignancies. Like the blocking antibodies, IFNγKO CAR T cells had reduced production of IFNγ but maintained Granzyme B expression and effectively lysed tumor cells *in vitro* (Fig. 3A and B). Tumor-bearing mice treated with IFNγKO CAR T cells exhibited reduced serum IFNγ levels but similar tumor clearance, engraftment, and survival as KO CAR T-cell–treated mice

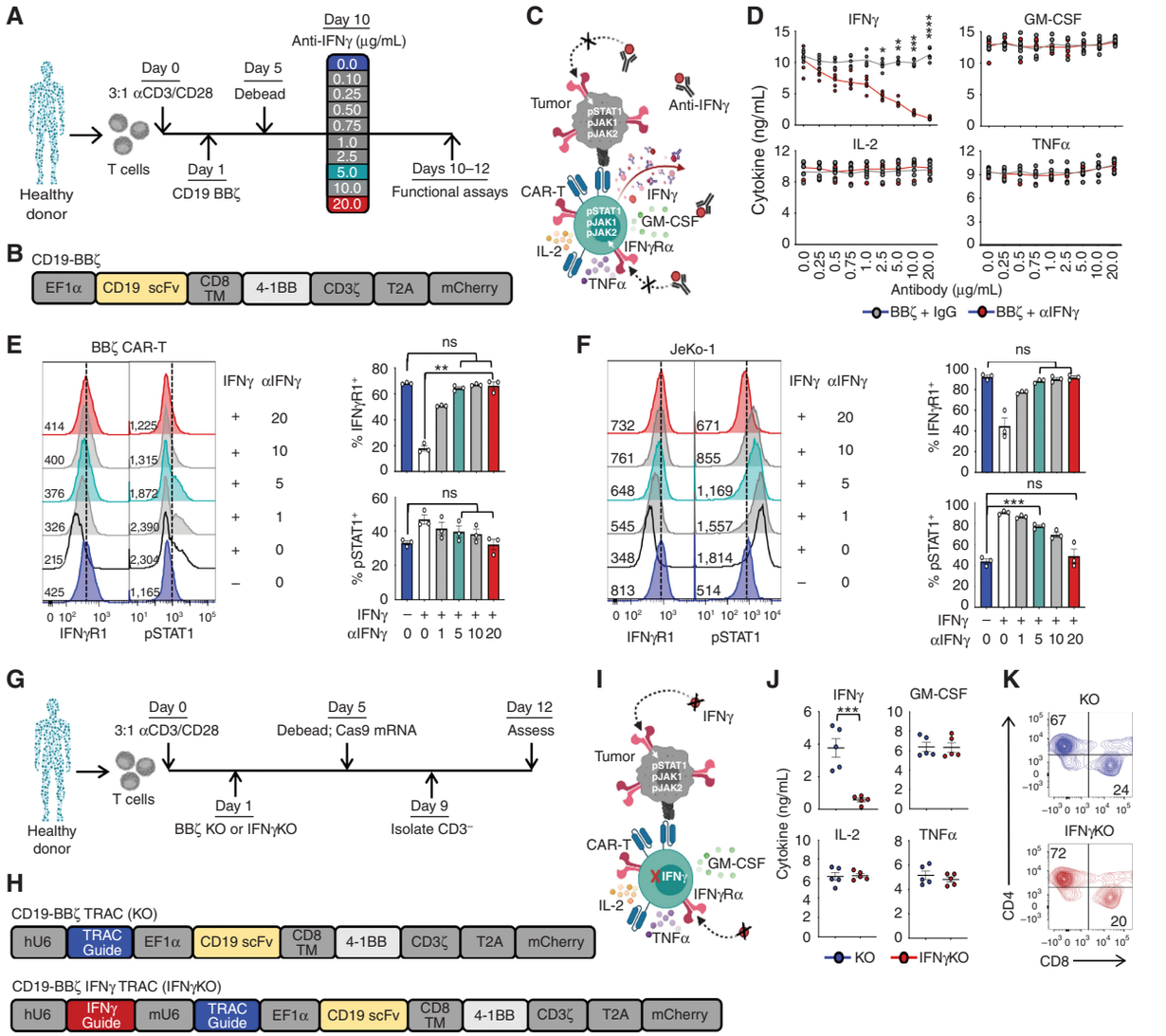

Figure 1. IFNγ can be pharmacologically and genetically blocked in CAR T cells. **A–C,** CAR T cells were generated from healthy donors, and IFNγ signaling was disrupted using αIFNγ-blocking antibodies. scFV, single-chain variable fragment. TM, transmembrane domain. **D,** BBζ CAR T cells were activated with phorbol 12-myristate 13-acetate (PMA)/ionomycin in the presence of αIFNγ antibody or IgG control and assessed by ELISA; $n = 5$. **E** and **F,** IFNγR1 and pSTAT1 expression in CAR T (**E**) and JeKo-1 (**F**) lymphoma cells treated with (+) or without (–) 10 ng/mL IFNγ ± αIFNγ-blocking antibody (μg/mL) as shown by mean fluorescence intensity (left) and percentage of positive cells (right); $n = 3$. **G–I,** BBζ CAR T cells genetically lacking TRAC (KO) or TRAC and IFNγ (IFNγKO) were generated from healthy donors. **J,** KO and IFNγKO CAR T cells were activated with PMA/ionomycin and assessed by ELISA; $n = 5$. **K,** CD4 and CD8 populations were determined by flow cytometry (representative of $n = 5$). Data are shown as mean ± SEM with P values by unpaired t tests (**D** and **J**) or one-way ANOVA (**E** and **F**). *, $P < 0.05$; **, $P < 0.01$; ***, $P < 0.001$; ****, $P < 0.0001$; ns, not significant.

using both lymphoma (Fig. 3C–H) and leukemia (Fig. 3I–N) mouse models. Given that CD19-specific CAR T cells utilizing a CD28 costimulatory domain (28ζ) can also produce IFNγ and mediate toxicities and responses in patients, we next assessed whether IFNγ is required for tumor clearance by 28ζ CAR T cells. We generated KO and IFNγKO CAR T cells with a CD28 costimulatory domain (Supplementary Fig. S3A) and assessed their cytotoxic capacity against Nalm6 leukemia cells. Like BBζ KO CAR T cells, IFNγ KO had no impact on cytotoxicity against leukemia cells by 28ζ CAR T cells (CAR-T) *in vitro* (Supplementary Fig. S3B), and other than having reduced levels of IFNγ in serum (Fig. 3O and P), IFNγ KO did not behave differently than IFNγ-replete CAR T cells *in vivo* (Fig. 3Q). These data confirm that IFNγ production by CAR T cells appears to be dispensable for effective BBζ and 28ζ CAR T-cell function in the setting of CD19$^+$ malignancies.

Given the established role of IFNγ as a marker of T-cell effector function, the finding that it is dispensable for effective cytotoxicity against CD19$^+$ tumor cells was surprising. To determine whether this was isolated to tumors expressing CD19, we next generated CAR T cells specific for the B-cell maturation antigen (BCMA), which is now an established target in multiple myeloma (Supplementary Fig. S3C). Specific antibody-mediated blockade of IFNγ production and not

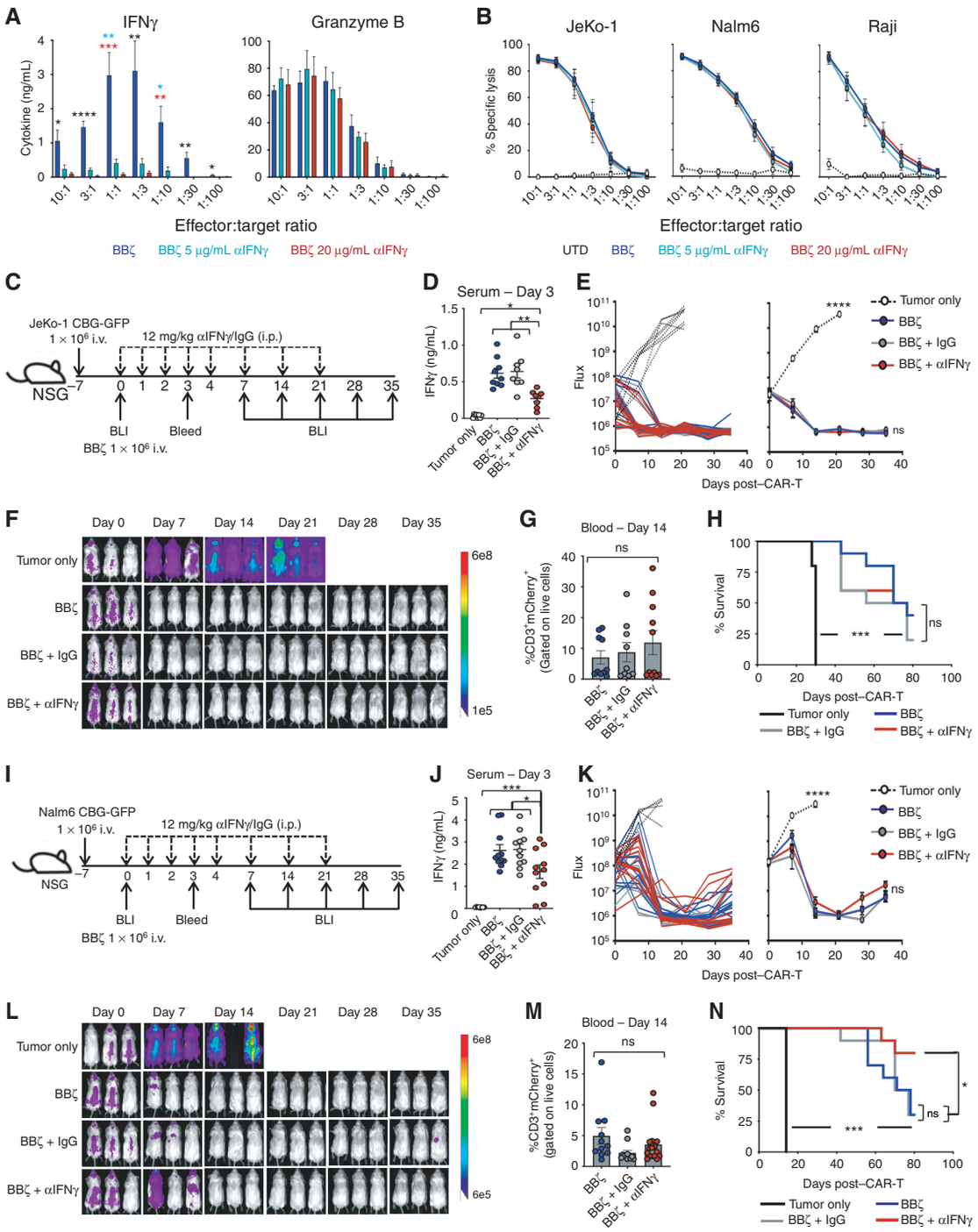

Figure 2. IFNγ blockade does not diminish CAR T-cell efficacy *in vitro* or *in vivo*. **A,** BBζ CAR T cells were combined with Nalm6 tumor cells overnight at various effector:target ratios in αIFNγ-blocking antibody (0, 5, 20 μg/mL), and IFNγ and Granzyme B production was determined by ELISA; $n = 5$. **B,** Luciferase-based specific lysis of JeKo-1, Nalm6, and Raji tumor cells by BBζ CAR-T with αIFNγ-blocking antibodies; $n = 5$. **C–H,** NSG mice were intravenously injected with JeKo-1 tumor cells and treated with BBζ CAR T cells ± αIFNγ or IgG control antibodies as shown in **C**. IFNγ expression in serum collected from mice 3 days posttreatment with BBζ CAR ± antibodies (**D**). Tumor growth was tracked by bioluminescent imaging (BLI; **E** and **F**), CAR T persistence in the blood was determined on day 14 post-CAR injection (**G**), and overall survival was monitored throughout (**H**). **I–N,** Experiments described in **C–H** were repeated using the Nalm6 tumor model. For all experiments, $n = 3$–5 mice/group; repeated with 3 healthy donors. Data are shown as mean ± SEM with P values by one-way ANOVA or log-rank (Mantel–Cox test) for Kaplan–Meier curves. *, $P < 0.05$; **, $P < 0.01$; ***, $P < 0.001$; ****, $P < 0.0001$; ns, not significant.

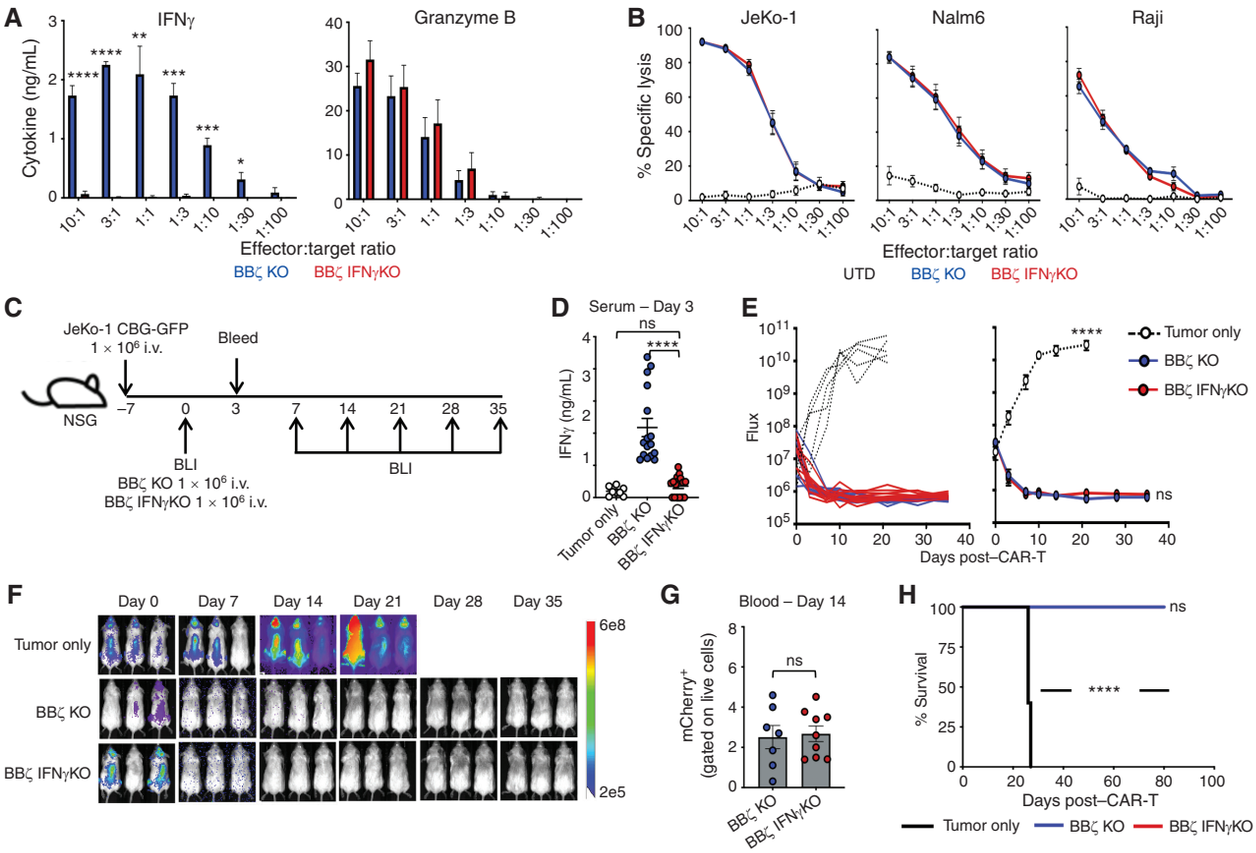

Figure 3. IFNγKO CAR T-cell clear lymphoma and leukemia tumors *in vitro* and *in vivo*. **A,** BBζ KO/IFNγKO CAR T cells were combined with Nalm6 tumor cells overnight at various effector:target ratios, and IFNγ and Granzyme B production was determined by ELISA; $n = 5$. **B,** Luciferase-based specific lysis of JeKo-1, Nalm6, and Raji tumor cells by BBζ KO/IFNγKO CAR T cells, $n = 5$. **C–H,** NSG mice were intravenously injected with JeKo-1 tumor cells and treated with BBζ KO or IFNγKO CAR T cells as shown in **C**. IFNγ expression in serum collected from mice 3 days posttreatment with BBζ CAR T cells (**D**). Tumor growth was tracked by bioluminescent imaging (BLI; **E** and **F**), CAR T-cell persistence in the blood was determined on day 14 post–CAR injection (**G**), and overall survival was monitored throughout (**H**). (*continued on next page*)

other cytokines was confirmed using BCMA BBζ CAR T cells cocultured with the BCMA-expressing multiple myeloma cell line RPMI-8226 at various effector-to-target (E:T) ratios (Supplementary Fig. S3D). As with leukemia and lymphoma tumors, loss of IFNγ had no impact on *in vitro* cytotoxicity against two different myeloma cell lines, either by antibody blockade (Supplementary Fig. S3E) or by IFNγ genetic KO (Supplementary Fig. S3F); these data suggest that IFNγ production by CAR T cells does not have an essential role in mediating cytotoxicity against hematologic malignancies.

Although the role of IFNγ in CAR T-cell therapy for hematologic malignancies has not been previously reported, it is thought to play a role in solid tumors. To determine whether IFNγ production by CAR T cells impacts cytotoxicity against solid tumors in similar assays, we generated KO and IFNγKO CAR T cells targeting mesothelin antigen with the SS1 single-chain variable fragment and assessed their capacity to lyse the pancreatic adenocarcinoma cell line BxPC-3 and Capan-2 tumor cells in overnight and real-time killing assays (Supplementary Fig. S3G–S3I). We found that pancreatic tumor lines had moderate resistance to mesothelin-targeted CAR T cells in the absence of IFNγ. Similarly, we found that antibody blockade of IFNγ dampened cytotoxicity of anti-EGFR CAR T cells against the EGFR$^+$ glioblastoma cell line U87 *in vitro* (Supplementary Fig. S3J and S3K). Collectively, these data suggest that IFNγ may have differential impacts on antitumor efficacy of CAR T cells in hematologic versus solid malignancies.

IFNγ KO Reduces Immune Checkpoint Proteins and Increases 28ζ CAR T-cell Proliferation

On the basis of previous reports of IFNγ upregulating immune checkpoint proteins, such as programmed cell death protein 1 (PD-1; ref. 4) and CTLA4 (5), we next sought to evaluate how the loss of IFNγ would affect the expression profile of immune checkpoint proteins in CAR T cells. Given that innate immune cells, such as macrophages, amplify the IFNγ signal and could thereby increase its upregulation of immune checkpoint proteins, we assessed how the loss of IFNγ in CAR T cells affects their phenotype in the absence and presence of macrophages. To do this, we generated KO and IFNγKO CAR T cells from healthy donors, cocultured them with Nalm6 leukemia cells at an E:T ratio of 1:10 with or without donor-matched GM-CSF–activated macrophages for 5 days, and assessed for

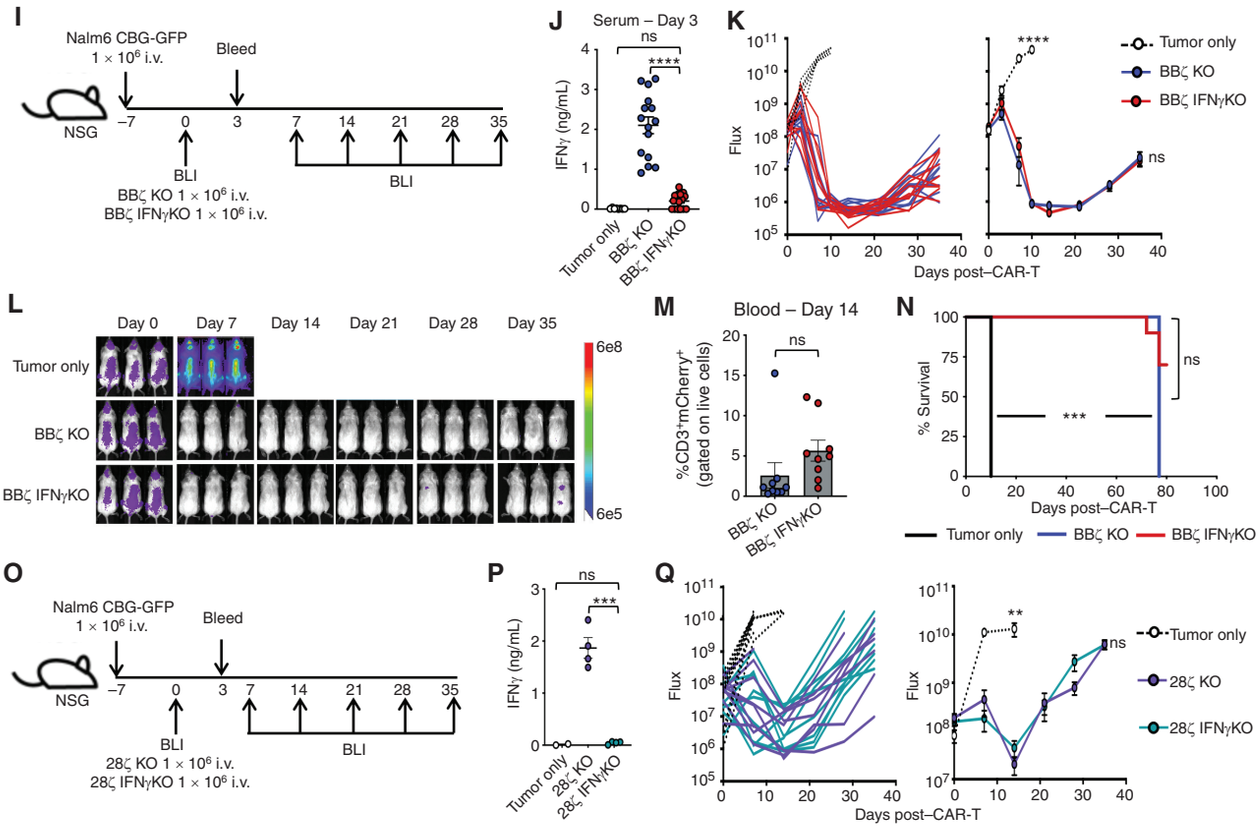

Figure 3. ***(Continued)*** **I–N,** Experiments described in **C–H** were repeated using the Nalm6 tumor model. **O–Q,** NSG mice were intravenously injected with Nalm6 tumor cells and treated with 28ζ KO or IFNγKO CAR T cells (**O**). Mice were assessed for IFNγ in the serum (**P**) and measured weekly using bioluminescence (**Q**). For BBζ experiments, $n = 3$–5 mice/group; repeated with 3 healthy donors. For 28ζ experiment, $n = 5$ mice/group; repeated with 2 healthy donors. Data are shown as mean ± SEM with P values by one-way ANOVA or log-rank (Mantel–Cox test) for Kaplan–Meier curves. *, $P < 0.05$; **, $P < 0.01$; ***, $P < 0.001$; ****, $P < 0.0001$; ns, not significant.

immune checkpoint proteins and CAR T-cell proliferation. Regardless of macrophage presence, IFNγKO BBζ CAR T cells had similar proliferative capacity as KO CAR T cells (Supplementary Fig. S4A) but exhibited a slightly reduced expression of the immune checkpoint proteins Lag3, PD-1, and Tim3, as shown by lower mean intensity (Supplementary Fig. S4B) and frequency (Supplementary Fig. S4C), particularly in the CD4$^+$ subset of macrophage-treated cultures.

On the basis of previous preclinical and clinical data, CAR T cells containing the CD28 costimulatory domain have greater antigen sensitivity and cytotoxic activity but increased inhibitory proteins and reduced persistence compared with CAR T cells containing the 4-1BB costimulatory domain (18, 19); therefore, we next sought to determine how 28ζ CAR T cells are affected by the loss of IFNγ. In contrast to BBζ CAR T cells, IFNγKO 28ζ CAR T cells had significantly greater expansion compared with KO CAR T cells in the absence and presence of macrophages (Supplementary Fig. S4D). We further found that IFNγKO CD4$^+$ and CD8$^+$ CAR T cells had reduced upregulation of PD-1, Tim3, and Lag3 compared with KO CAR T cells (Supplementary Fig. S4E and S4F), regardless of the presence or absence of macrophages in the culture. The percentage of Lag3-, PD-1–, and Tim3-expressing CAR T cells was consistently lower in the IFNγ-deficient group, although it was only statistically significant for Tim3 in CD4$^+$ T cells. Altogether, these data reveal that IFNγ plays a role in the upregulation of immune checkpoint proteins on CAR T cells and suggests that IFNγ signaling restricts the expansion of CAR T cells, especially those with CD28 signaling domains.

Establishing Macrophage Activation Models to Mimic Patient Cytokine Profiles

Given the role of IFNγ in innate immune activation (1, 2) and the correlation between high IFNγ serum levels and CRS/macrophage activation syndrome (MAS) in the clinic (20, 21), we next sought to determine if the absence of IFNγ could mitigate CAR-mediated macrophage activation. We have treated patients with lymphoma with either tisagenlecleucel or axicabtagene ciloleucel CAR-T products and have collected toxicity data and serum samples early in their course under an Institutional Review Board (IRB)–approved protocol. We selected serum samples from patients who later went on to develop cytokine-related toxicities, namely CRS, MAS, or ICANS, in the first 2 weeks after CAR T-cell infusion (Fig. 4A). Cytokine profiles were first measured from serum samples collected 2 to 5 days postinfusion, prior to treatment with tocilizumab, steroids, and/or anakinra (in all but one patient who received tocilizumab early)

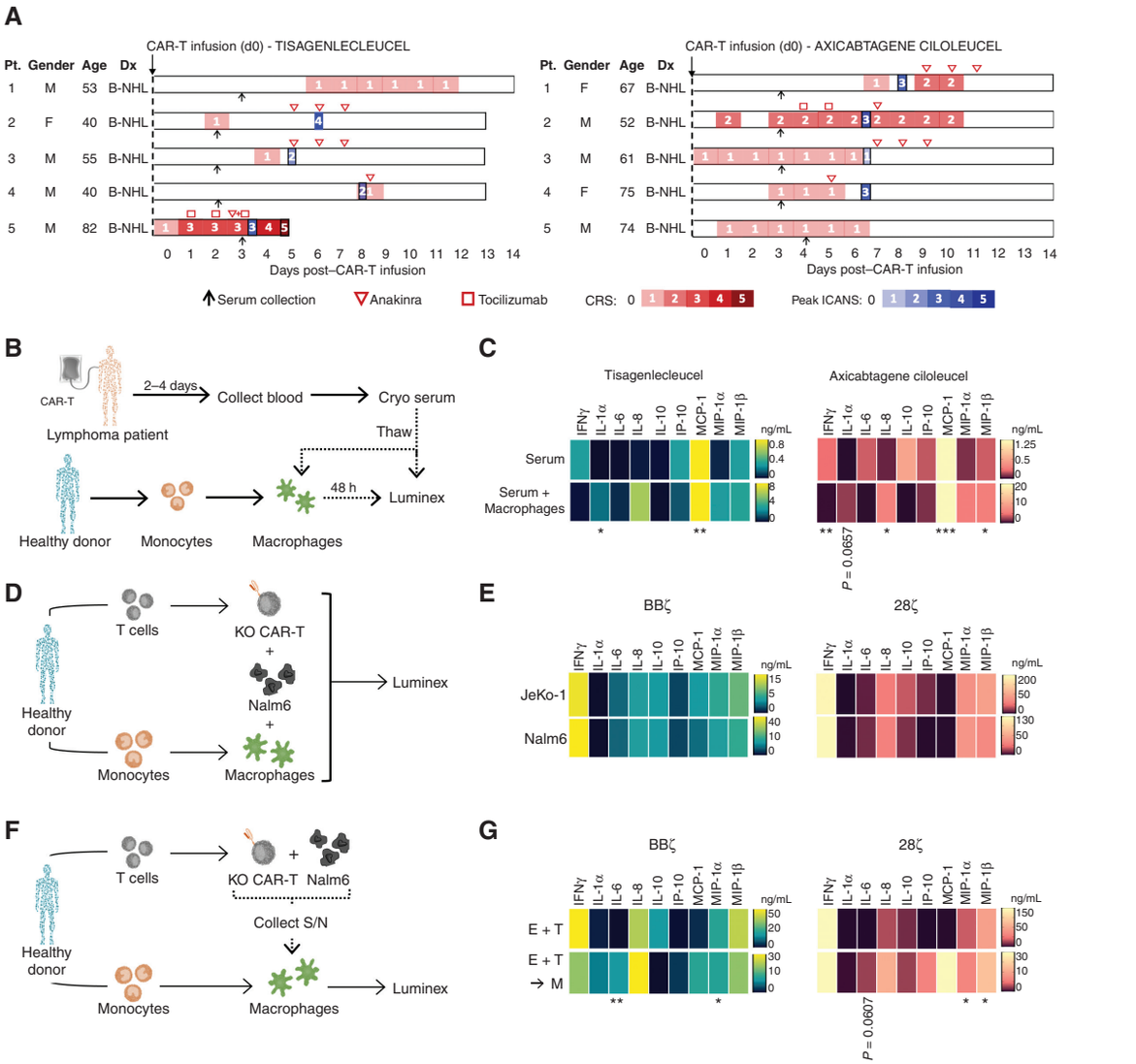

Figure 4. Establishing macrophage activation models to simulate lymphoma patient cytokine profiles. **A,** Swimmer plots for patients with lymphoma in this study, including dates of serum collection (black arrow), anakinra treatment (red inverted triangle), tocilizumab treatment (red square), CRS grading (red gradient), and peak ICANS days (blue gradient). B-NHL, B-cell non-Hodgkin lymphoma; Dx, diagnosis. **B** and **C,** Serum from patients receiving tisagenlecleucel or axicabtagene ciloleucel CAR T-cell products was collected 2 to 5 days post-CAR treatment and added to healthy donor–derived GM-CSF–activated macrophages; cytokines were assessed 48 hours later. Luminex data were graphed by heat map to highlight upregulated proteins in serum alone (top) and following addition to macrophages (bottom) in tisagenlecleucel and axicabtagene ciloleucel patients; $n = 5$ patients/CAR T-cell product. **D** and **E,** Healthy donor BBζ and 28ζ KO CAR T cells were generated and combined at a 1E:1T:0.02M ratio with donor-matched macrophages and JeKo–Nalm6 or JeKo-1 cells for 48 hours, and serum was analyzed by Luminex ($n = 5$). **F** and **G,** Healthy donor KO CAR T cells were generated and combined with Nalm6 at a 1:1 ratio overnight before serum was collected and added to donor-matched macrophages for 48 hours. Serum from the E:T cultures (top) and E:T:M (bottom) was collected, analyzed by Luminex, and graphed by BBζ (left) or 28ζ (right), $n = 5$. S/N, supernatant. Data are shown as heat maps depicting mean values with P values by unpaired t tests. *, $P < 0.05$; **, $P < 0.01$; ***, $P < 0.001$.

to avoid skewing cytokine profiles after cytokine-directed interventions. Serum cytokines were graphed individually (Supplementary Fig. S5A and S5B) and by mean total (Supplementary Fig. S5C and S5D). In agreement with previous studies, patients with documented CRS and/or ICANS had elevations in IFNγ, IL-6, IL-10, IP-10, MCP-1, and MIP-1β as compared with control patients who did not experience CRS or ICANS. Of note, CXCL9 and CXCL10 (IP-10) are both driven by IFNγ, upregulated in patients with HLH and CRS (12), and reduced following clinical administration of the IFNγ-blocking antibody emapalumab (refs. 22–24; CXCL9 was not included in our Luminex panel).

Our goal was to mimic the patient cytokine profile *in vitro* using T cells and monocytes/macrophages from healthy donors. CAR T cells made from these donors were cocultured with Nalm6 tumor cells, and their supernatants, which contain cytokines produced during CAR T-cell activation, were collected. Monocytes from the same donors were left untreated or differentiated into various macrophage subsets (M0, M1, M2, GM-CSF–activated) and exposed to

donor-matched supernatant from the CAR-T:Nalm6 cocultures. On the basis of comparing the cytokine profiles after supernatant exposure to our patients' serum cytokine profiles, GM-CSF–activated macrophages were the closest match, with increased IL-6, IP-10, and MCP-1 production compared with baseline (Supplementary Fig. S6A–S6C). We then further developed the GM-CSF macrophages as an *in vitro* model of human CAR T-cell–induced CRS. To determine how GM-CSF–activated macrophages responded to circulating cytokines from patients who had developed CAR T-cell–induced CRS, we added serum from the axicabtagene ciloleucel– or tisagenlecleucel-treated patients directly to healthy donor–derived macrophages for 48 hours and then measured the cytokine profiles by Luminex (Fig. 4B; of note, the sample from the patient who had received tocilizumab prior to serum collection was excluded in this experiment due to the effect of tocilizumab on measurements of IL-6). Macrophage cultures exposed to serum from patients who went on to develop cytokine-mediated toxicities after axicabtagene ciloleucel or tisagenlecleucel exhibited an elevated production of IL-1α, IL-8, IP-10, MCP-1, MIP-1α, and MIP-1β (Fig. 4C; mean values), all of which were absent or reduced in macrophage cultures treated with control patient samples (no CRS; Supplementary Fig. S6D; mean values).

To build fully *in vitro* models that could recapitulate the macrophage activation cytokine profiles from patients, we refined our GM-CSF macrophage activation system to test *in vitro* CAR-T/tumor interactions into contact-dependent (CAR T + tumor cells + macrophages) and contact-independent (CAR T + tumor cells → supernatant to macrophages) culture systems. We first confirmed macrophage activation in the contact-dependent model by identifying increased expression of the inflammatory proteins IL-1α, IL-6, and IP-10 and the T-cell cytokines IFNγ, IL-8, and IL-10 compared with CAR T-cell and tumor cell cultures alone (Supplementary Fig. S7A). Contact-dependent cultures with control KO BBζ and KO 28ζ CAR T cells yielded broad macrophage activation, as defined by elevated levels of IFNγ, IL-6, IL-8, IL-10, IL-13, MCP-1, MIP-1α, and MIP-1β in response to both Nalm6 and JeKo-1 target cells (Fig. 4D and E). Due to the similarity between the two cell lines, and for simplicity, we chose to move forward with just the Nalm6 leukemia model. For the contact-independent approach, supernatant from Nalm6:KO CAR T-cell cultures was added to donor-matched macrophages and assessed for cytokine secretion (Fig. 4F). Like the first model, both BBζ and 28ζ KO CAR T cells elicited strong macrophage responses, as seen by increased production of IL-1α, IL-6, IL-8, IP-10, MCP-1, MIP-1α, and MIP-1β (in E+T→M cultures), compared with CAR T-cell and tumor cell cultures alone (E+T; Fig. 4G). Both *in vitro* approaches showed similar cytokine expression patterns to the patient samples, especially following macrophage addition. Although neither approach exactly recapitulated the profile of every patient sample, all the upregulated cytokines and chemokines identified in these models have been reported in patients with CRS. Therefore, these *in vitro* systems provide a rapid, robust, and scalable model of CAR T-cell–induced macrophage activation, which we could then leverage to assess the role of IFNγ in catalyzing cytokine-related toxicities, and as well as to measure the effects of other drugs and downstream cytokine pathways.

IFNγ-Deficient CAR T Cells Reduce Macrophage Activation in a Contact-Independent Manner

Prior to determining how IFNγ augments macrophage activation, we confirmed the generation of mature macrophages based on the upregulation of CD86 and inducible nitric oxide synthase (iNOS; Fig. 5A). Next, we sought to verify that IFNγ could trigger measurable IFNγ receptor signaling in GM-CSF–activated macrophages by showing increased phosphorylation of JAK1 and STAT1 in response to recombinant human IFNγ (Fig. 5B). To determine how the loss of IFNγ affects the contact-dependent cell culture model introduced in Fig. 4B, donor-matched KO or IFNγKO CAR T cells were cocultured with $CD19^+$ Nalm6 cells plus or minus donor-matched GM-CSF–activated macrophages and supernatant was collected at 6, 24, 48, and 72 hours (Supplementary Fig. S7B–S7E). Cytokine analysis of BBζ and 28ζ cultures revealed that while KO and IFNγKO CAR T cells had similar inflammatory profiles in the absence of macrophages (Supplementary Fig. S7C), macrophage-containing IFNγKO cultures exhibited decreased activation/function, as shown by lower levels of IL-1β, IL-6, IP-10, and MCP-1 (Supplementary Fig. S7E).

To determine whether this reduction in macrophage activation was contact-dependent, supernatant from CAR-T:Nalm6 cocultures was added to donor-matched GM-CSF–activated macrophages for 48 hours, and then resulting supernatants were collected and analyzed for cytokines (Fig. 5C). Like our initial coculture system, we found that macrophage activation was diminished when using supernatant from either BBζ or 28ζ IFNγKO CAR T-cell cultures, suggesting that this effect is not contact-dependent (Fig. 5D and E). To confirm that the reduced levels of cytokines/chemokines in these cultures was specifically and mechanistically due to the loss of IFNγ, we added an IFNγ-blocking antibody to KO CAR T cells or added recombinant IFNγ to IFNγKO CAR-T cultures to see whether the macrophage phenotypes could be reversed simply by the deletion or addition of IFNγ. We found that manipulation of IFNγ alone was able to reverse the functional profile of macrophages in both BBζ (Fig. 5F and G) and 28ζ (Fig. 5H and I) cultures, as shown by mean total expression (Fig. 5F and H) and fold change (Fig. 5G and I), thereby confirming the dominant role of IFNγ in macrophage response to CAR T-cell activation.

In addition to measuring cytokine production as a functional assay of macrophage activation, we confirmed reduced activation of macrophages in response to BBζ and 28ζ IFNγKO CAR T cells by measuring surface expression of the macrophage activation markers CD86 and CD69 and downstream IFNγ signaling (pJAK1, pJAK2, pSTAT1; Fig. 5J and K; Supplementary Fig. S8A and S8B). Furthermore, macrophages treated with IFNγKO CAR T cells showed reduced expression of the checkpoint inhibitory molecule programmed death ligand 1 (PD-L1). Overall, these data further confirm that CAR T cells induce macrophage activation in an IFNγ-dependent manner.

Although two murine *in vivo* CRS models have been reported, these approaches are quite challenging, not only because of the need to start with large numbers of T cells to account for CRISPR editing and isolation of successful KO

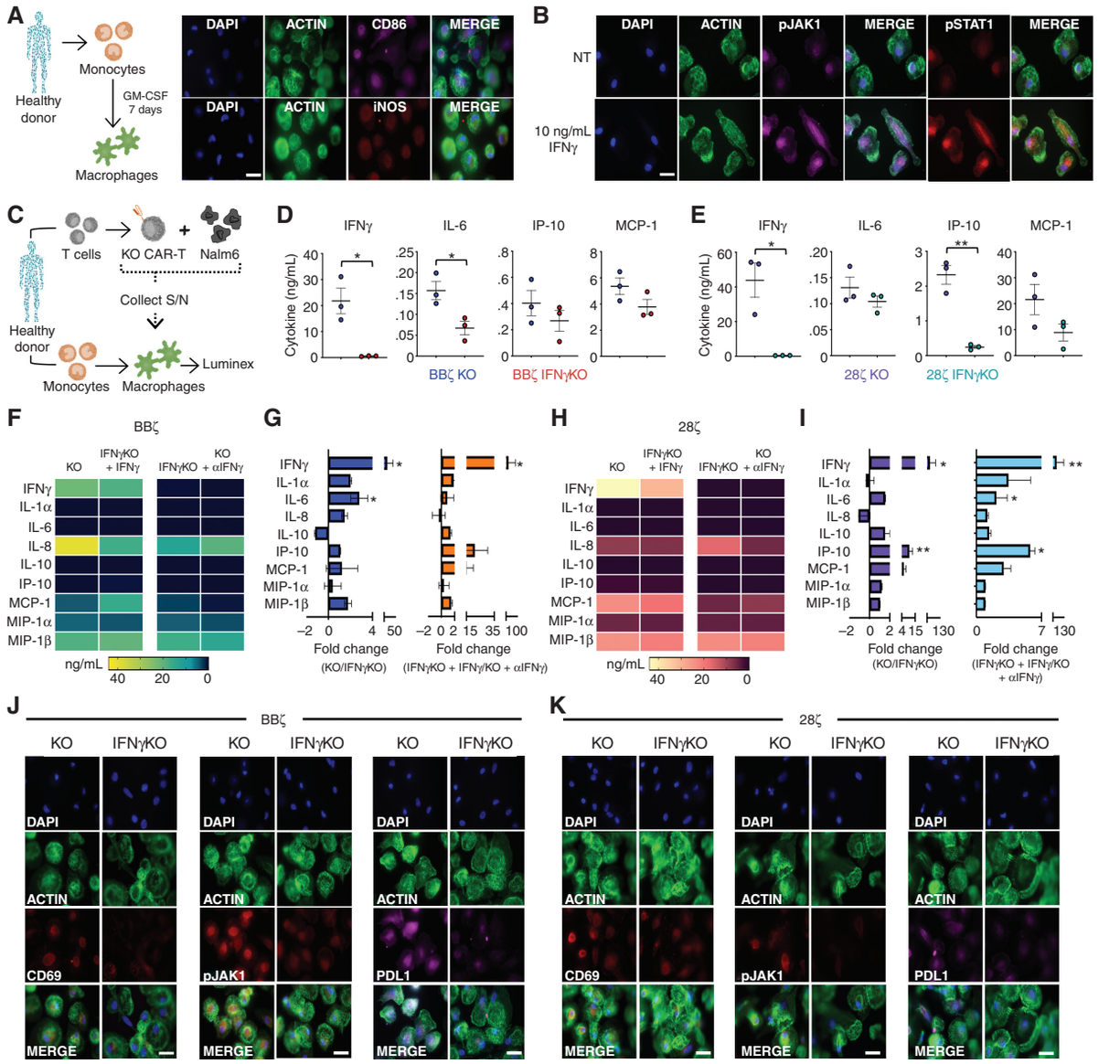

Figure 5. IFNγKO CAR T cells reduce macrophage activation in a contact-independent manner. **A,** Monocytes were isolated from healthy donors and expanded to generate GM-CSF–activated macrophages prior to immunofluorescence staining; representative of $n = 2$ (magnification 63×). Scale bars, 10 μm. **B,** GM-CSF–activated macrophages were generated in healthy donors and left untreated (NT; top) or given 10 ng/mL recombinant human IFNγ (bottom) for 4 hours prior to staining for pJAK1 and pSTAT1 by fluorescent microscopy; representative of $n = 2$ (magnification 63×). Scale bars, 10 μm. **C–E,** KO/IFNγKO CAR T cells were generated from healthy donors and combined with Nalm6 cells for 24 hours prior to supernatant (S/N) collection and addition to donor-matched GM-CSF–activated macrophages (**C**). Forty hours later, supernatant was collected from macrophages, and function was assessed by Luminex for BBζ (**D**) and 28ζ (**E**); $n = 3$. **F** and **G,** Using the protocol from **C**, supernatant from BBζ cultures was added to macrophages and left untreated, or IFNγKO CAR T cells were given 10 ng/mL recombinant human IFNγ and KO CAR T-cell supernatant was supplemented with 20 μg/mL αIFNγ-blocking antibody. Cytokines were assessed by Luminex and graphed as a heat map of mean expression (**F**) and fold change (**G**; $n = 5$). **H** and **I,** Using the protocol from **C**, supernatant from 28ζ cultures was added to macrophages and left untreated or IFNγKO CAR T cells were given 10 ng/mL recombinant human IFNγ and KO CAR T-cell supernatant was supplemented with 20 μg/mL αIFNγ-blocking antibody. Cytokines were assessed by Luminex and graphed as a heat map of mean expression (**H**) and fold change (**I**; $n = 5$). Macrophages from cultures in **D** and **E** were fixed and stained for CD69, pJAK1, and PD-L1 for both BBζ (**J**) and 28ζ (**K**); representative of $n = 2$ (magnification 63×). Scale bars, 10 μm. Data are shown as mean ± SEM with P values by unpaired t tests. *, $P < 0.05$; **, $P < 0.01$.

CAR T cells (25), but because of the lack of cross-reactivity between human and mouse IFNγ (26). Therefore, we sought to establish a hybrid *in vivo/in vitro* model in which macrophage activation could be assessed. To this end, serum from Nalm6-bearing, KO CAR T-cell–treated, or IFNγKO CAR T-cell–treated mice was added to donor-matched macrophages *in vitro* and then profiled by Luminex (Fig. 6A). At baseline, mouse serum (prior to its addition to macrophages) had slightly higher but not significant (aside from IFNγ) cytokine levels after treatment with KO CAR T cells

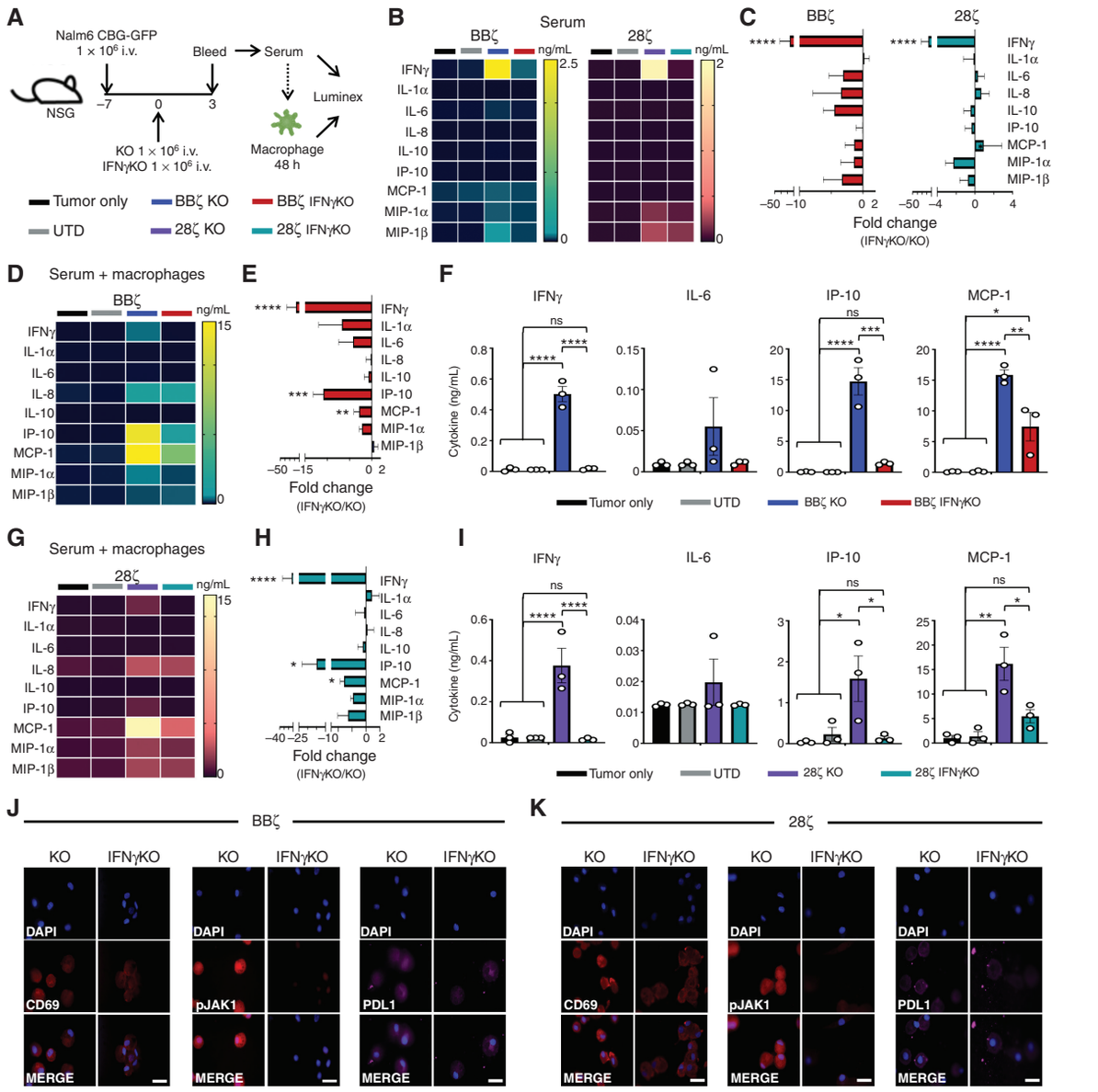

Figure 6. Serum from tumor-bearing mice treated with IFNγKO CAR T cells yield reduced macrophage responses *in vitro*. NSG mice were intravenously injected with Nalm6 tumor cells and left untreated (tumor only) or given UTD or KO/IFNγKO CAR T cells. Three days post-CAR injection, serum was collected and used directly for Luminex assessment or added to donor-matched macrophages. Forty-eight hours later, supernatant was collected and assayed for cytokine expression. **A,** Schematic of experimental layout. **B** and **C,** Serum from BBζ and 28ζ CAR–treated mice collected directly from mice was assayed by Luminex and graphed by mean values (**B**) and fold-change expression (**C**). **D–I,** Serum from mice was added to macrophages for 24 hours prior to collection and Luminex assessment for BBζ (**D**–**F**) and 28ζ (**G**–**I**) groups. Data are shown as mean value (**D** and **G**), fold-change expression (**E** and **H**), and cytokine level (**F** and **I**). **J** and **K,** Following supernatant collection, macrophages were stained for CD69, pJAK1, and PD-L1 expression for both BBζ (**J**) and 28ζ (**K**) subsets (magnification 63×). Scale bars, 10 μm. Experiments were performed in 3–5 mice/group and repeated with 4 healthy donors. Data in **C**, **E**, and **H** are shown as mean ± SEM with *P* values by unpaired *t* tests. Data in **F** and **I** are shown as mean ± SEM with *P* values by one-way ANOVA. *, $P < 0.05$; **, $P < 0.01$; ***, $P < 0.001$; ****, $P < 0.0001$; ns, not significant.

compared with those treated with UTD, IFNγKO CAR T cells, or mice with tumor alone (Fig. 6B and C). However, the differences in cytokine profiles among the groups were further amplified when mouse serum was added to donor-matched GM-CSF–activated macrophages. In particular, the macrophage activation–associated cytokines identified in our patients with lymphoma (IL-6, IP-10, MCP-1, MIP-1α) were elevated when adding sera from KO CAR T-cell–treated mice compared with IFNγKO CAR T cells in both BBζ (Fig. 6D–F) and 28ζ (Fig. 6G–I) cultures. Fluorescent imaging confirmed reduced macrophage activation, IFNγ receptor signaling, and PD-L1 expression in macrophages exposed to BBζ or 28ζ IFNγKO CAR T cells (Fig. 6J and K; Supplementary Fig. S8C and S8D). We also noted that the absolute levels of human cytokines recovered from mouse sera were much lower than in the supernatants recovered from *in vitro* cocultures of

CAR T cells with tumor cells (as indicated by the scales in the heat maps of Fig. 4 compared with Fig. 6). However, the levels of human cytokines recovered from mouse sera were closer in scale to the concentrations recovered from human patients. Thus, using hybrid mouse/human mixed *in vivo/in vitro* models enabled us to evaluate macrophage activation in response to CAR T-cell therapies and demonstrate the principal role of IFNγ in this interplay.

IFNγ Blockade Reduces Macrophage Activation to a Greater Extent than Current Clinical Biologic Approaches

We next wanted to compare how targeting IFNγ in CAR T cells would compare to current clinical practices for treating CRS and macrophage activation, which are typically based on blocking IL-6R (ref. 27; tocilizumab) or IL-1 (ref. 28; with anakinra, an IL-1RA competitor). To this end, we leveraged our contact-independent coculture system and used blocking antibodies against IFNγ, IL-1Rα, and IL-6R in cultures of macrophages with conditioned media from IFNγ-replete BBζ or 28ζ CAR T cells cocultured with $CD19^+$ targets (Supplementary Fig. S9A). Cultures treated with αIFNγ blockade showed significant reduction in IFNγ, IL-1α, IL-8, and IP-10 as well as slightly reduced levels of IL-6 and MCP-1 compared with no treatment or traditional anti–IL-1Rα and anti–IL-6R blocking strategies (Supplementary Fig. S9B). Although we primarily chose to focus on GM-CSF–activated macrophages due to their cytokine profile, we verified that IFNγ-deplete CAR T-cell cultures yielded reduced macrophage activation (as measured by IL-6 production) in M0, M1, M2, and mixed macrophage populations similar to that of the GM-CSF–activated subset (Supplementary Fig. S9C). While macrophages play a role in the development of CRS (26), it has also been reported that monocyte-derived IL-1 and IL-6 contribute to CRS and neurotoxicity (25, 29). To determine how IFNγ inhibition affects monocyte function, we repeated these experiments using donor-matched monocytes and saw a reduction of IFNγ, IL-6, IP-10, and MCP-1 using both BBζ and 28ζ CAR constructs (Supplementary Fig. S9D and S9E). Overall, these data suggest that blocking IFNγ reduces macrophage and monocyte activation at least as well as if not more than current clinical approaches.

Finally, we sought to determine how various blocking antibodies would affect the macrophage response to serum collected from patients with B-cell lymphoma treated with tisagenlecleucel or axicabtagene ciloleucel CAR T-cell products (introduced in Fig. 4). We used these serum samples and added it to healthy donor GM-CSF–activated macrophages in the absence or presence of blocking antibodies. Macrophage responses after 48 hours were assessed by measuring cytokine production and targeted RNA sequencing (Fig. 7A). We found that blocking IFNγ in sera from tisagenlecleucel patients led to similar macrophage responses compared with blockade of IL-1Rα (αIL-1Rα) and IL-6R (αIL-6R), with additional reductions in IFNγ, IL-1α, IL-6, and IP-10 (Fig. 7B; Supplementary Fig. S10A). Serum collected from the patient who had already received three doses of tocilizumab prior to collection (orange dot) revealed increased expression of IP-10 that was reduced only by IFNγ blockade. Furthermore, all patients had increased IL-6 levels following αIL-6R blockade *in vitro*. Given the likely role of IL-6 in ICANS (25, 30), which can be especially elevated in patients treated with tocilizumab (31) and is simulated herein, these data highlight the potential for IFNγ blockade to manage or prevent both CRS and ICANS.

Transcriptional analysis revealed a distinct profile of differentiated genes for macrophages treated with serum from tisagenlecleucel-treated patients in the presence of IL-6R–, IL-1Rα–, or IFNγ-blocking antibodies compared with control macrophages devoid of antibody blockade [Supplementary Fig. S10B; Supplementary Data (NanoString sequencing data)]. Pathway scoring in tisagenlecleucel patients showed strong clustering between no treatment/αIL-6R as well as between αIFNγ/αIL-1Rα (Fig. 7C; Supplementary Fig. S10C), with the former group having heightened angiogenesis and extracellular matrix (ECM) remodeling pathways compared with αIFNγ and αIL-1Rα. While macrophages treated with patient serum plus αIL-1Rα or αIFNγ blockade clustered together, these subsets maintained distinct transcriptional profiles (Supplementary Fig. S10D). Building on our previous findings showing that IFNγ affects immune checkpoint protein expression, αIFNγ-treated macrophages exhibited upregulation of costimulatory genes, including *DPP4* and *ICOSLG* (Fig. 7D; Supplementary Fig. S10E and S10F), which have been implicated in enhanced CAR T-cell therapy (32, 33), and a reduction of coinhibitory genes such as *HAVCR2* and *PDCD1LG2* (Fig. 7E; Supplementary Fig. S10G). Similar findings occurred in cultures treated with sera from patients who received axicabtagene ciloleucel, with an additional reduction of MIP-1β (Fig. 7F–I; Supplementary Fig. S10H–S10N). Collectively, these data reveal that IFNγ blockade could reduce macrophage activation and potentially mitigate major cytokine-related toxicities (CRS, MAS, and ICANS) in the clinic. Furthermore, blocking IFNγ increased costimulatory genes and reduced immune checkpoint genes to a similar or greater extent than current clinical approaches, which could enhance CAR T-cell function and persistence in patients, thus improving both the efficacy and toxicity profiles of this powerful therapy.

DISCUSSION

Although IFNγ production is frequently used as a measure of antigen-specific T-cell and CAR T effector cell function and potency, we hypothesized and demonstrated that IFNγ production was not essential for antitumor efficacy in hematologic malignancies. Our findings are supported by recent data from Singh and colleagues, who reported that in an unbiased genome-wide CRISPR screen of Nalm6 leukemia cells, defects in programmed cell death pathways mediated resistance to CAR T-cell–mediated cytotoxicity (34), but there was no evidence for a role of IFNγR or its signaling pathway proteins in conferring resistance to CD19-directed CAR T cells. We focused on hematologic malignancies for testing our hypothesis on the role of IFNγ because these are the currently approved and successful indications for CAR T cells and where the incidence and severity of cytokine-related toxicities are clinically significant. We recognize that IFNγ may play a different role in solid tumors based on data presented here as well as in other emerging work from our laboratory that identified IFNγ receptor signaling as a resistance pathway in solid tumors (10).

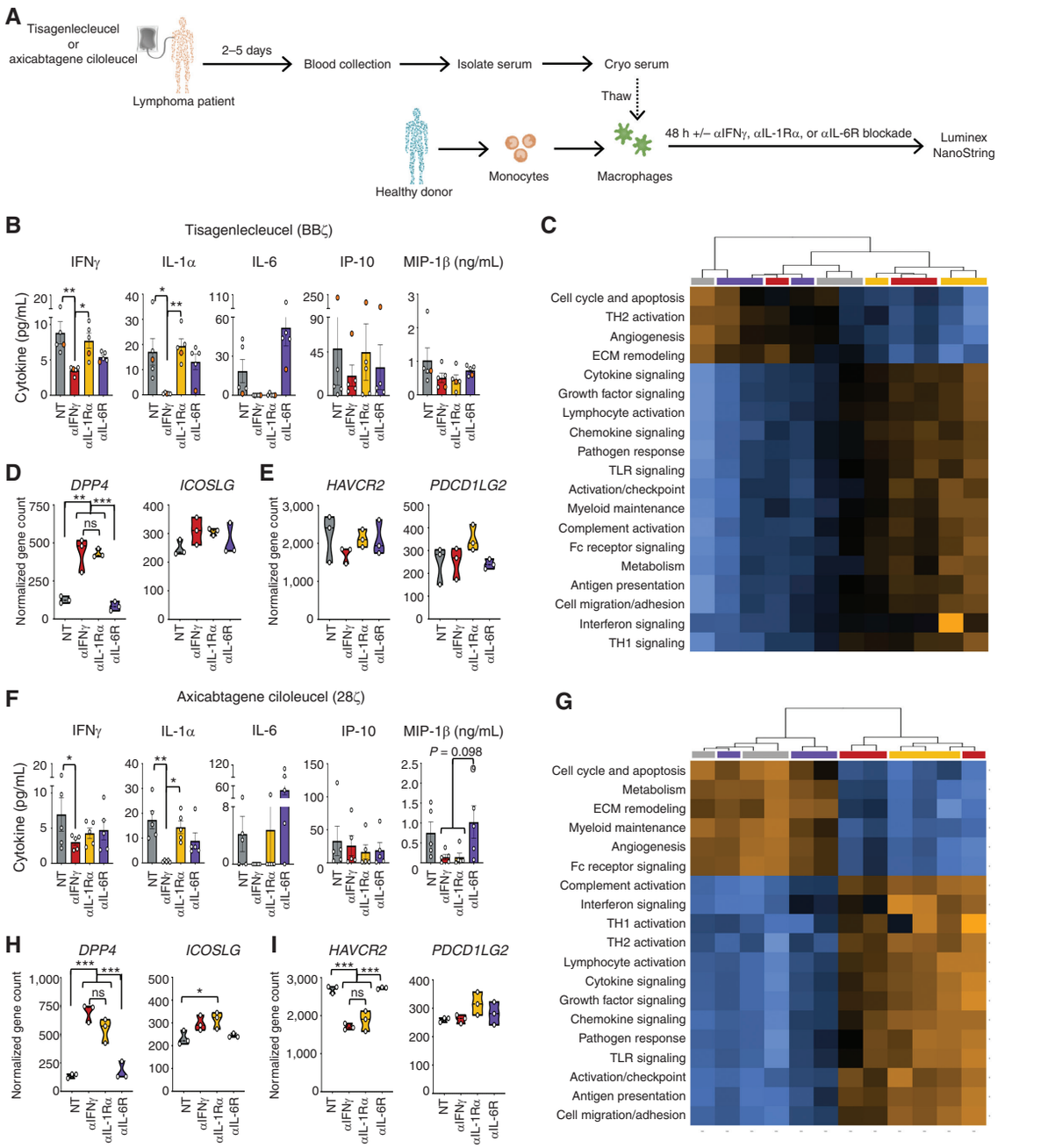

Figure 7. Blocking IFNγ reduces macrophage activation in lymphoma patients to a greater extent than current biological approaches. **A,** Serum from patients receiving tisagenlecleucel or axicabtagene ciloleucel CAR T-cell products was collected 2 to 5 days post-CAR treatment, added to healthy donor-derived GM-CSF–activated macrophages ± blocking antibodies to IFNγ, IL-1Rα, and IL-6R, and were assessed 48 hours later. **B–F,** Cultures receiving serum from tisagenlecleucel patients were assessed by Luminex (**B**) or NanoString (**C–E**). Experiments above were repeated using serum from axicabtagene ciloleucel (**F–I**). NanoString analysis for both groups was graphed as pathway score heat maps (**C** and **G**) and normalized gene counts (**D**, **E**, **H**, and **I**). Data are shown as mean ± SEM with *P* values by one-way ANOVA. *, $P < 0.05$; **, $P < 0.01$; ***, $P < 0.001$; ns, not significant.

Our data also reveal that despite being dispensable for direct cytotoxicity of CAR T cells, IFNγ plays two major roles in this context: (i) IFNγ dampens T-cell proliferation, especially in CAR T cells containing a CD28 costimulatory domain, and mediates upregulation of inhibitory checkpoint proteins, and (ii) IFNγ drives macrophage activation and subsequent production of proinflammatory cytokines/chemokines. Checkpoint blockade therapy has been combined with CAR T-cell therapy to increase CAR T-cell persistence with modest effects (35, 36), and combinations of IL-1R and IL-6R blockades have been used to mitigate clinical toxicities driven by macrophage activation (37, 38). Data herein suggests that both of these goals, of reducing immune checkpoint proteins and macrophage activation, could be

simultaneously accomplished by blocking or deleting IFNγ. In this study, we found that immune checkpoint protein expression was reduced, but not absent, on both BBζ and 28ζ IFNγKO CAR T cells; however, this only translated to a significantly greater *in vitro* proliferation in 28ζ CAR T cells. These findings suggest that while IFNγ depletion could enhance CAR T-cell survival and persistence via reduced immune checkpoints, there are most likely additional factors driving the rapid growth of 28ζ CAR T cells. We recognize that clinically, reduction of immune checkpoint proteins also has the potential to elicit or amplify toxicities not driven by IFNγ and its downstream effects (39). In addition, *in vivo* antibody blockade of IFNγ would be expected to affect all T cells, not just CAR T cells, and may result in increased susceptibility to infections.

The strength of our work lies in the use of dual, nonoverlapping approaches (antibody blockade and genetic deletion) to specifically examine the role of a single cytokine; the use of CAR T cells bearing both costimulatory domains that are in widespread use (4-1BB and CD28); the use of multiple specificities, target antigens (CD19, BCMA, EGFR, mesothelin), and tumor histologies (leukemia and lymphoma, multiple myeloma, glioblastoma, and pancreatic adenocarcinoma, respectively); and the development of novel, scalable, and robust models of *in vitro* and hybrid *in vivo/in vitro* macrophage activation that were optimized to mimic cytokine profiles from patient-derived samples. Although we did not test the impact of IFNγ blockade or deletion in immunocompetent models, recent work from the Fry lab showed that blocking IFNγ in an immunocompetent mouse model of leukemia did not diminish tumor clearance in mice treated with wild-type CAR T cells, supporting our findings (40). Our work focused on the interaction of CAR-produced IFNγ with macrophages and monocytes; however, IFNγ is known to interact with other cells, including stromal and endothelial cells (41), which were not tested herein. While immunocompetent mouse models would allow us to more fully test the impact of IFNγ on other hematopoietic cells and nonhematopoietic tissues, the differences in human and murine biology, in addition to those in tumor-associated antigens and CAR constructs for these species, may not provide a true picture of the biology most relevant to human patients. For example, syngeneic models do not develop the clinical syndrome of CRS the way patients do (e.g., mice do not develop fever or measurable hypotension or cognitive dysfunction), and the lack of cross-reactivity with IFNγ/IFNγR makes it especially difficult to study this specific axis in mice (26).

A sophisticated humanized model of CRS has been published (25), but the complexities inherent to this model have made it challenging for widespread implementation; one finding from this model was that IFNγ was one of the most upregulated cytokines that led to enhanced production of IL-1 and IL-6. Here, we focused on evaluating more scalable *in vitro* and hybrid models that could best recapitulate the cytokine and chemokine profiles observed in patients as they develop CRS (i.e., IFNγ, IL-6, IP-10, MCP-1, MIP-1β) and that have been previously correlated clinically with cytokine-mediated syndromes, including CRS, MAS, and HLH (12). On the basis of various *in vitro* models testing cocultures and supernatants from CAR T cells with tumors and macrophages that had been derived from monocytes through various differentiation protocols (including monocytes, M0, M1, M2, and GM-CSF–stimulated macrophages), we found that the *in vitro* culture system using supernatants from CAR T cells cultured with tumor cells, added to GM-CSF–macrophages, best recapitulated the cytokine profiles observed in patients; our hybrid model, using sera from tumor-bearing mice treated with CAR T cells, also replicated the cytokine profiles from patients when added to GM-CSF macrophages, but generally produced lower levels of IL-6 than the *in vitro* models, likely due to lower overall concentrations of human IFNγ recovered from mouse sera. Although no model perfectly recapitulates the human clinical toxicity, we are optimistic that these *in vitro* and hybrid models will prove to be useful, scalable, and of interest to the field.

In vitro comparisons of IFNγ blockade or KO in the CAR T-cell product with currently used clinical strategies suggested that targeting IFNγ could mitigate major cytokine-related toxicities to a greater extent than existing approaches. Although early intervention with tocilizumab did not interfere with CAR T-cell efficacy in clinical trials, it also did not prevent or ameliorate neurotoxicity, and inflammatory cytokines such as IFNγ and MIP-1β remained elevated (37). A clinical trial using prophylactic administration of tocilizumab was found to reduce severe CRS but increased neurotoxicity, likely due to elevated IL-6, which tocilizumab does not reduce (38). While clinical trials are still ongoing, an early report on the use of anakinra prophylaxis in patients with multiple myeloma treated with CAR T cells reported fewer grade 2 events in patients and reduced the need for corticosteroids, but the overall frequency of CRS was similar to the nonrandomized control group, although there were no grade 3 or higher events reported (42). Collectively, these studies reveal that although early/prophylactic intervention with antibodies targeting the IL-1 and IL-6 pathways do not diminish CAR T-cell efficacy, they may not entirely mitigate CRS or neurotoxicity. A recent study has suggested that like IFNγ, upstream activators of macrophage activation, such as GM-CSF, can be targeted to reduce CAR-mediated toxicities (43). While a direct comparison between IFNγ and GM-CSF blockade was initially planned herein, only 3 of the 12 patients in this study had detectable GM-CSF in their sera, suggesting that this cytokine may not be a key mediator of CRS in our sample of patients with lymphoma.

There has been understandable hesitation to administer IFNγ-blocking antibodies to patients with severe cytokine-related toxicities, especially since these are frequently reversible with existing clinical measures, and because the risk of abrogating an antitumor response in patients with relapsed or refractory disease has been considered high. Furthermore, blocking antibodies to IFNγ received their first and only FDA approval in November 2018, for primary HLH, and they are still expensive and difficult to obtain for off-label uses. Our data suggest that IFNγ may not be critical for CAR T-cell efficacy in hematologic malignancies but could mitigate cytokine-related toxicities by reducing macrophage/monocyte activation and function, specifically IL-1α, IL-6, IP-10, and MCP-1. In agreement with our hypothesis, recent clinical work by McNerney and colleagues revealed that IFNγ blockade can mitigate CRS in CAR T-cell–treated patients without

compromising antitumor efficacy (17). Our data suggest that IFNγ deletion from CAR T-cell products is a specific and viable strategy that could improve CAR T-cell efficacy and also prevent or mitigate cytokine-related toxicities in hematologic malignancies.

METHODS

CAR Design

Four CAR constructs (two anti-CD19, one anti-BCMA, and one anti-EGFR) were synthesized and cloned into a second-generation lentiviral backbone under the regulation of a human EF-1α promoter. For CD19, one construct contained a CD8 transmembrane domain in tandem with an intracellular 4-1BB costimulatory domain and a CD3ζ signaling domain (BBζ), while the second was identical, but with a CD28 costimulatory domain replacing 4-1BB (28ζ). For BCMA and EGFR constructs, the CD8 transmembrane domain was in tandem with intracellular 4-1BB and a CD3ζ signaling domain. Eight additional constructs were created as described above but containing guide RNA sequences for TRAC (AGAGTCTCTCAGCTG GTACA) ± IFNγ (CCAGAGCATCCAAAAGAGTG). Pilot studies were performed using multiple guide RNA sequences from the Brunello library (44) to each target, but only the most effective guides were used for the final constructs, including TRAC (AGAGTCTCTCAGCTGG TACA) and IFNγ (CCAGAGCATCCAAAAGAGTG). Using these guide sequences, KO and IFNγKO CAR constructs were made to target CD19 (two with 4-1BB and two with CD28), BCMA (two with 4-1BB), and mesothelin (two with 4-1BB). All constructs contained a transgene coding the fluorescent reporter mCherry to determine transduction.

CRISPR/Cas9 Guide Selection

The IFNγ-producing T-cell line SMZ-1 was transduced to constitutively express CBG-GFP and stable Cas9 with puromycin resistance for selection. Four IFNγ-targeted guides (G1 = CCAGAGCATCCA AAAGAGTG, G2 = TGAAGTAAAAGGAGACAATT, G3 = TGCAG GTCAGATGTAG, G4 = TTCTCTTGGCTGTTACTGC) were purchased from the Brunello library (ref. 44; Broad Institute, Cambridge, MA) and assessed for their ability to knock out IFNγ in SMZ-1 cells. A GFP guide was used as a control to verify Cas9 activity and rule out nonspecific IFNγ targeting by knocking out GFP in SMZ-1 cells without affecting IFNγ production. Two of the four guides (G1 and G2) deleted IFNγ production in SMZ-1 cells compared with UTD and GFP control. These guides were incorporated into CAR constructs, and although both specifically reduced IFNγ production in the SMZ-1 cell line, only guide 1 effectively reduced IFNγ in primary CAR T cells; therefore, this guide was chosen for further studies.

CAR T-cell Production

Human T cells were isolated from the peripheral blood of anonymous healthy donor leukapheresis product (Stem Cell Technologies) purchased from the Massachusetts General Hospital (MGH) blood bank under an IRB-approved protocol. T cells were resuspended in R10 media (RPMI1640 + 10% FBS + penicillin/streptomycin) supplemented with 20 IU/mL IL-2 and activated using anti-CD3/CD28 Dynabeads (Life Technologies) at a 1T:3B ratio. Twenty-four hours postactivation, T cells were transduced with one of the lentiviral vectors encoding anti-CD19, BCMA, mesothelin, or EGFR CAR constructs described above. Cells were debeaded 5 days postactivation and expanded in the presence of 20 IU/mL IL-2. For KO CAR T cells, T cells were resuspended at 5×10^6/100 μL in Opti-MEM (Thermo Fisher Scientific) after debeading on day 5 and electroporated with 10 μg Cas9 mRNA (TriLink) at 360V × 001 ms. Three to five days later, $CD3^-$ T cells were isolated by column purification (EasySep Human APC Positive Selection Kit II; STEMCELL Technologies) or flow-based cell sorting using the BD FACSAria. Deletion of CD3 (TRAC) and IFNγ was confirmed by flow cytometry and ELISA. Transduction efficiency was determined using mCherry expression by flow cytometry. For all functional assays, CAR T cells and KO CAR T cells were normalized for transduction efficiency.

Mice and Cell Lines

NSG mice were purchased from The Jackson Laboratory and bred under pathogen-free conditions at the MGH Center for Comparative Medicine (Boston, MA). All experiments were performed according to protocols approved by the MGH Institutional Animal Care and Use Committee. The human SMZ-1, JeKo-1, Nalm6, Raji, MM.1S, RPMI-8226, BxPC-3, Capan-2, and U87 cell lines were purchased from ATCC. All cell lines were authenticated and regularly tested for *Mycoplasma*. Cell lines were engineered to constitutively express click beetle green luciferase (CBG) and enhanced GFP (GFP) prior to sorting on FACSAria (BD Biosciences) to obtain a ≥99% CBG-GFP^+ population. SMZ-1, JeKo-1, Nalm6, Raji, MM.1S, RPMI-8226, and BxPC-3 cell lines were cultured in R10 media (RPMI1640 + 10% FBS + penicillin/streptomycin). Capan-2 and U87 cell lines were cultured in D10 media (DMEM + 10% FBS + penicillin/streptomycin).

Blocking Antibodies

IFNγ was pharmacologically blocked with 0.1 to 20 μg/mL purified NA/LE mouse anti-human IFNγ clone NIB42 or control anti-IgG1 mouse isotype control clone 107.3 (BD Biosciences). Blocking and control antibodies were refreshed every 24 hours as needed. To block IL-1Rα and IL-6R, Il-1rα monoclonal antibody (10309; Thermo Scientific) and tocilizumab (Selleck Chemicals) were added to cultures at 10 μg/mL and 5 μg/mL, respectively, and refreshed every 24 hours as needed.

ELISA

CAR T cells were activated for 6 hours using Cell Activation Cocktail without Brefeldin A (BioLegend) or at varying E:T ratios with target (Nalm6, JeKo-1, MM.1S, RPMI-8226) cells for 18 hours, and supernatant was collected. Cytokine levels of IFNγ, IL-2, GM-CSF, TNFα, and Granzyme B were measured according to manufacturer's protocol using Human DuoSet ELISA kits (R&D Systems).

Flow Cytometry

The following antibodies were purchased for flow cytometry from BioLegend: CCR6-PE/Cy7 (clone G034E3), CD3-APC (clone OKT3), CD45RO-APC, CD62L-FITC (clone DREG-56), CTLA-4-PE/Cy7 and CXCR3-BV421; BD Biosciences: CD4-v450 (clone SK3), CD8-v500 (clone SK1), Lag3-AF647 (clone T47–530), PD-1-BV786 (clone EH12.1) and Tim3-BV711 (clone 7D3); R&D Systems: CCR4-AF488; Abcam: IFNγR1 (clone EPR7866); and Thermo Fisher Scientific: DAPI. For extracellular staining, cells were stained in the dark for 20 minutes at room temperature in BD Horizon Brilliant Stain Buffer (BD Biosciences) and washed twice with FACS Buffer (PBS + 2% FBS) prior to acquisition. To measure viability, cells were left untreated or activated nonspecifically through Cell Activation Cocktail (BioLegend) for 6 hours or in an antigen-specific manner using $CD19^+$ Nalm6 target cells at a 1:1 ratio for 18 hours. DAPI was added to cultures at 1:500 and analyzed immediately. Cells to be saved for analysis at later time points were fixed using Fixation Buffer (BioLegend) according to protocol. For phosphoflow, cells were resuspended at 1×10^6/mL and left untreated, treated with αIFNγ (1–20 μg/mL), and/or given 10 ng/mL recombinant human IFNγ (BioLegend) for 20 minutes at 37°C. Cells were fixed at a 1:1 ratio with BD Cytofix (BD Biosciences) for 15 minutes at room temperature. Following centrifugation, cells were resuspended in Perm Buffer III (BD Biosciences) at 2×10^6/mL, vortexed vigorously, and put on ice for 30 minutes. Cells were stained

with PhosphoStat1 Tyr701 (Clone 58D6; Cell Signaling Technology) in 1% PBSA followed by anti-rabbit IgG (H+L) and F(ab')2 Fragment AF647 (Cell Signaling Technology). All cells were run on a Fortessa X-20 (BD Biosciences) and analyzed using FlowJo software.

NanoString

CAR T cells were combined with Nalm6 cells at a 1E:10T ratio for 5 days. Remaining cells were collected, and CAR T cells ($mCherry^+GFP^-$) were isolated using flow-based sorting on the BD FACSAria. For patient samples, serum was added to GM-CSF–activated macrophages in culture in the presence or absence of blocking antibodies to IFNγ, IL-1Rα, or IL-6R for 48 hours. CAR T cells from Nalm6 cultures and macrophages from patient cultures were lysed using RLT buffer to obtain RNA, and code set probes were hybridized with RNA by PCR for 18 hours at 65°C according to NanoString protocol. nCounter gene expression assays (NanoString Technologies) were performed using NanoString XT CAR-T Panel Standard + Customized PLUS panel (CAR-T) or nCounter Myeloid Innate Immunity Panel (macrophages). Hybridized RNA was loaded into nCounter MAX cartridges, run on the nCounter MAX and quantified using nSolver or nSolver Advanced software. For advanced analysis, donors/patients as covariates were considered. Normalized data were used for $\log_2$ scores, and gene counts are shown herein.

In Vitro *Killing Assays*

For single time-point cytotoxicity assays, CAR T cells were incubated with luciferase-expressing target cells at the indicated E:T ratios for 18 hours. Remaining luciferase activity was measured using the Luciferase Assay System (Promega) with a Synergy Neo2 luminescence microplate reader (Biotek). Percent specific lysis was calculated using the following equation: % Specific lysis = [(total relative luminescence units (RLU)/target cells only RLU) × 100]. For real-time cytotoxicity assays using plate-bound (via CD9) Nalm6 cells, cell index was recorded as a measure of cell impedance using the xCELLigence RTCA SP instrument (ACEA Biosciences). Graphs for percent cytolysis were calculated on the ACEA software to show percent target killing by CAR T-cell groups compared with tumor only.

NSG Xenograft Models

Six- to 8-week-old male and female NSG mice were intravenously injected with 1×10^6 JeKo-1 or Nalm6 CBG-GFP^+ cells. Seven days later, mice were randomized and left untreated (tumor only) or intravenously injected with 1×10^6 CAR T cells, and tumor burden was measured by bioluminescence using an Ami spectral imaging apparatus and analyzed with IDL software following intraperitoneal injection of D-Luciferin substrate solution (30 mg/mL; no blinding). Mice receiving IFNγ-blocking antibody (InVivoMab anti-human IFNγ; Bio X Cell) or control IgG (InVivoMab mouse IgG1 isotype control; Bio X Cell) were intraperitoneally injected with 12 mg/kg of the appropriate solutions 1 hour prior to CAR T-cell injection. Antibodies were readministered intraperitoneally every 24 hours for the first 5 days and then maintained with 1 injection per week through day 21. For most experiments, mice were bled on days 3 and 14 post–CAR T-cell injection to monitor IFNγ expression/cytokine profiles and CAR T-cell persistence, respectively. In all experiments, bioluminescence was measured weekly.

Incucyte

Healthy donor–derived KO and IFNγKO CAR T cells targeting CD19 were combined with Nalm6 leukemia cells at 10:1, 1:1, or 1:10 E:T ratios with or without donor-matched GM-CSF–activated macrophages, and proliferation of $mCherry^+$ CAR T cells was assessed for 5 days on the Incucyte. Anti-CD19 28ζ KO and IFNγKO CAR T cells were cultured at a 1:1 ratio with Nalm6 cells, and tumor burden (GFP) was monitored for 5 days. Anti-mesothelin BBζ KO and IFNγKO CAR T cells were cultured at a 1:1 ratio with BxPC-3 or Capan-2 cells, and tumor burden (GFP) was monitored for 5 days.

Innate Cell Isolation and Differentiation

Peripheral blood mononuclear cells were isolated from healthy donors using Ficoll-Paque PLUS (GE Healthcare, C987R36), and monocytes were purified with a kit from StemCell (19359). Recombinant human carrier-free cytokines were purchased from BioLegend (GM-CSF and IFNγ), Shenandoah Biotechnology (IL-4, IL-13, and M-CSF), and Sigma-Aldrich (lipopolysaccharide, LPS). Monocytes were plated and differentiated into various macrophage subsets as described previously (45): M0 (25 ng/mL M-CSF), GM-CSF–activated (5 ng/mL GM-CSF), M1 (5 ng/mL GM-CSF, 20 ng/mL IFNγ, 100 ng/mL LPS), and M2 (25 ng/mL M-CSF, 20 ng/mL IL-4, 20 ng/mL IL-13). Following macrophage differentiation, cocultures with donor-matched CAR T and/or target cells were constructed as described below and in figure legends. For all cultures, macrophages were left on original plates and washed briefly with PBS prior to the addition of CAR T cells and/or tumor cells. The ratio of 50 CAR-T: 1 macrophage or monocyte was consistent throughout experiments and was based on previous work (29).

CAR T-cell, Macrophage, and Tumor Cocultures

For contact-dependent studies, donor-matched macrophages were generated, CAR T cells/target cancer cells were added at varying tumor quantities—low (10E:1T:0.02M), moderate (1E:1T:0.02M), or high (1E:10T:0.02M)—and supernatant was collected for analysis at 6, 24, 48, or 72 hours. CAR T cell plus macrophage cultures were included as a control and exhibited a similar functional profile as CAR T cell alone. For contact-independent studies, CAR T and Nalm6 cells were cultured at a 1:1 ratio overnight. After 24 hours, supernatant was collected and added to donor-matched GM-CSF–activated macrophages for 48 hours prior to supernatant collection and analysis.

Luminex

Supernatant was collected from cocultures as denoted in figure legends, and cytokine production was measured using the Human Inflammatory Panel 20-plex ProcartaPlex Panel (Thermo Fisher Scientific) and run on the FLEXMAP 3D System (Luminex).

Macrophage Activation from Mouse Serum

Six- to 8-week-old male and female NSG mice were intravenously injected with 1×10^6 JeKo-1 or Nalm6 CBG-GFP^+ cells. Seven days later, mice were randomized and left untreated (tumor only) or intravenously injected with 1×10^6 KO/IFNγKO CAR T cells, and tumor burden was measured by bioluminescence as described above (no blinding). Serum was collected from mice 3 days post–CAR T-cell injection and either saved for Luminex or added directly to donor-matched GM-CSF–activated macrophages in culture. Forty-eight hours later, supernatant was collected and assessed for function using the Human Inflammatory Panel 20-plex Luminex kit and macrophages were imaged using fluorescence microscopy.

Fluorescence Microscopy

Monocytes from healthy donors were plated on iBidi glass-bottom 8-well slides and kept in 5 ng/mL GM-CSF for 7 days prior to use. Recombinant human IFNγ, supernatant from CAR T-cell/tumor culture, or serum from mice was collected and added directly to washed macrophages for 48 hours. Cells were fixed and permeabilized using the Molecular Probes Image iT kit according to protocol (Thermo Fisher Scientific). Cells were stained with unconjugated primary antibodies, purchased from Thermo Fisher Scientific (CD69, CD86, PD-L1) or Cell Signaling Technology [pJAK1 (clone D7N4Z), pJAK2 (clone C80C3), pSTAT1 (clone 58D6), iNOS (clone D6B6S)],

overnight at a concentration of 1:100 to 1:200. Secondary anti-rabbit antibodies conjugated to AF647 or AF549 (Cell Signaling Technology) were used at 1:500 for detection. Molecular Probes Actin Green 488 (Thermo Fisher Scientific) was used for actin staining, and slides were mounted using Prolong Gold Antifade Reagent with DAPI (Cell Signaling Technology). Macrophages were imaged on the Zeiss Observer Microscope at 63× with similar exposures between all samples in each experiment.

Patient Samples

Annotated serum samples from patients with lymphoma treated with CAR T-cell products (tisagenlecleucel or axicabtagene ciloleucel) at our institution were obtained after written informed consent under a protocol (16–206) approved by the Dana-Farber/Harvard Cancer Center IRB. All patient samples used herein were collected 2 to 5 days after CAR T-cell infusion, and in all but one patient, collection was performed prior to treatment with tocilizumab or anakinra. Patient samples were assessed for cytokines/chemokines by Luminex or added to healthy donor macrophages (± blocking antibodies) *in vitro* for 48 hours prior to assessment.

Data Availability

The data generated in this study are available within the article and Supplementary Data files.

Statistical Analysis

All analyses were performed with GraphPad Prism v8 software. Data were presented as means ± SEM. with statistically significant differences determined by tests as indicated in figure legends. For experiments with multiple groups, correction for multiple comparisons was applied. All *n* values given are biologic replicates unless otherwise stated.

Authors' Disclosures

S.R. Bailey reports grants from NRSA T32 during the conduct of the study, as well as a patent for PCT/US2020/065733 pending. R.C. Larson reports grants from NIH during the conduct of the study. M. Wehrli reports grants from Swiss National Science Foundation (SNSF) during the conduct of the study, as well as a patent for CD89 activation in therapy issued to University of Bern and CSL Behring. M.V. Maus reports personal fees from 2Seventy Bio, TCR2, and Century Therapeutics outside the submitted work; a patent for PCT/US2020/065733 pending; multiple consulting relationships with companies developing and marketing cellular immune therapies, including consulting for Adaptimmune, Agenus, Arcellx, Astellas, AstraZeneca, Atara, Bayer, Bristol Myers Squibb, Cabaletta Bio (scientific advisory board), CRISPR Therapeutics, In8bio (scientific advisory board), Intellia, GlaxoSmithKline, Kite Pharma, Micromedicine, Novartis, Sanofi, TCR2 (scientific advisory board), Tmunity, Torque, and WindMIL and grant/research support from CRISPR Therapeutics, Kite Pharma, Servier, and Novartis; is a stockholder in Century Therapeutics, TCR2, and 2SeventyBio; and is a member of the board of directors for 2Seventy Bio. No disclosures were reported by the other authors.

Authors' Contributions

S.R. Bailey: Conceptualization, data curation, formal analysis, investigation, visualization, methodology, writing–original draft, writing–review and editing. **S. Vatsa:** Validation, investigation. **R.C. Larson:** Conceptualization, methodology, writing–review and editing. **A.A. Bouffard:** Data curation, validation, investigation. **I. Scarfo:** Conceptualization, methodology, writing–review and editing. **M.C. Kann:** Investigation, writing–review and editing. **T.R. Berger:** Writing–review and editing. **M.B. Leick:** Resources, visualization, writing–review and editing. **M. Wehrli:** Resources, visualization, writing–review and editing. **A. Schmidts:** Conceptualization, methodology, writing–review and editing. **H. Silva:** Investigation, writing–review and editing. **K.A. Lindell:** Resources, data curation. **A. Demato:** Resources, data curation. **K.M.E. Gallagher:** Resources, data curation. **M.J. Frigault:** Resources, data curation. **M.V. Maus:** Conceptualization, resources, formal analysis, supervision, funding acquisition, methodology, project administration, writing–review and editing.

Acknowledgments

We thank the following MGH Cancer Center core facilities for their assistance: Blood Bank and Pathology (Flow Cytometry and Imaging). We also thank the Immune Monitoring Laboratory in the MGH Cellular Immunotherapy Program, specifically Gabrielle Brini, Katelin Katsis and Jennifer Yam, for patient sample processing. We thank Korneel Grauwet for assisting with cell sorting. This work was supported by T32CA009216 (to S.R. Bailey), T32GM007306, T32AI007529, the Richard N. Cross Fund (to R.C. Larson), Lymphoma Research Foundation 612757 (to I. Scarfo), John Hansen Research Grant DKMS-SLS-JHRG-2020-04 (to A. Schmidts), T32CA071345-21A1 (to M.B. Leick), the Damon Runyon Cancer Research Foundation, a Stand Up To Cancer Innovative Research Grant, Grant Number SU2C-AACR-IRG 18-17, NIH R01CA252940, R01CA238268, and R01CA249062 (to M.V. Maus). Stand Up To Cancer is a division of the Entertainment Industry Foundation. The indicated Stand Up To Cancer grant is administered by the American Association for Cancer Research, the scientific partner of SU2C.

Note

Supplementary data for this article are available at Blood Cancer Discovery Online (https://bloodcancerdiscov.aacrjournals.org/).

Received October 7, 2021; revised November 10, 2021; accepted December 9, 2021; published first December 10, 2021.

REFERENCES

1. Kang K, Bachu M, Park SH, Kang K, Bae S, Park-Min KH, et al. IFN-gamma selectively suppresses a subset of TLR4-activated genes and enhancers to potentiate macrophage activation. Nat Commun 2019;10:3320.
2. Wu C, Xue Y, Wang P, Lin L, Liu Q, Li N, et al. IFN-gamma primes macrophage activation by increasing phosphatase and tensin homolog via downregulation of miR-3473b. J Immunol 2014;193:3036–44.
3. Garcia-Diaz A, Shin DS, Moreno BH, Saco J, Escuin-Ordinas H, Rodriguez GA, et al. Interferon receptor signaling pathways regulating PD-L1 and PD-L2 expression. Cell Rep 2017;19:1189–201.
4. Abiko K, Matsumura N, Hamanishi J, Horikawa N, Murakami R, Yamaguchi K, et al. IFN-gamma from lymphocytes induces PD-L1 expression and promotes progression of ovarian cancer. Br J Cancer 2015;112:1501–9.
5. Wang XB, Zheng CY, Giscombe R, Lefvert AK. Regulation of surface and intracellular expression of CTLA-4 on human peripheral T cells. Scand J Immunol 2001;54:453–8.
6. Scala E, Carbonari M, Del Porto P, Cibati M, Tedesco T, Mazzone AM, et al. Lymphocyte activation gene-3 (LAG-3) expression and IFN-gamma production are variably coregulated in different human T lymphocyte subpopulations. J Immunol 1998;161:489–93.
7. Song M, Ping Y, Zhang K, Yang L, Li F, Zhang C, et al. Low-dose IFNgamma induces tumor cell stemness in tumor microenvironment of non-small cell lung cancer. Cancer Res 2019;79:3737–48.
8. Karachaliou N, Gonzalez-Cao M, Crespo G, Drozdowskyj A, Aldeguer E, Gimenez-Capitan A, et al. Interferon gamma, an important marker of response to immune checkpoint blockade in non-small cell lung cancer and melanoma patients. Ther Adv Med Oncol 2018;10:1758834017749748.

9. Ayers M, Lunceford J, Nebozhyn M, Murphy E, Loboda A, Kaufman DR, et al. IFN-gamma-related mRNA profile predicts clinical response to PD-1 blockade. J Clin Invest 2017;127:2930–40.
10. Larson RC, Kann MC, Bailey SR, Haradhvala NJ, Stewart K, Bouffard AA, et al. Loss of IFNgR signaling and downstream adhesion confers resistance to CAR T-cell cytotoxicity in solid but not liquid tumors. Nature. In Press.
11. Grupp SA, Kalos M, Barrett D, Aplenc R, Porter DL, Rheingold SR, et al. Chimeric antigen receptor-modified T cells for acute lymphoid leukemia. N Engl J Med 2013;368:1509–18.
12. Teachey DT, Lacey SF, Shaw PA, Melenhorst JJ, Maude SL, Frey N, et al. Identification of predictive biomarkers for cytokine release syndrome after chimeric antigen receptor T-cell therapy for acute lymphoblastic leukemia. Cancer Discov 2016;6:664–79.
13. Fitzgerald JC, Weiss SL, Maude SL, Barrett DM, Lacey SF, Melenhorst JJ, et al. Cytokine release syndrome after chimeric antigen receptor T cell therapy for acute lymphoblastic leukemia. Crit Care Med 2017;45:e124–e31.
14. Maude SL, Barrett D, Teachey DT, Grupp SA. Managing cytokine release syndrome associated with novel T cell-engaging therapies. Cancer J 2014;20:119–22.
15. Arico M, Danesino C, Pende D, Moretta L. Pathogenesis of haemophagocytic lymphohistiocytosis. Br J Haematol 2001;114:761–9.
16. Maus MV, Leick MB, Cornejo KM, Nardi V. Case 35-2019: A 66-year-old man with pancytopenia and rash. N Engl J Med 2019;381:1951–60.
17. McNerney KO, DiNofia AM, Teachey DT, Grupp SA, Maude SL. Potential role of IFNγ inhibition in refractory cytokine release syndrome associated with CAR T-cell therapy. Blood Cancer Discov 2022;3:90–4.
18. Boroughs AC, Larson RC, Marjanovic ND, Gosik K, Castano AP, Porter CBM, et al. A distinct transcriptional program in human CAR T cells bearing the 4-1BB signaling domain revealed by scRNA-Seq. Mol Ther 2020;28:2577–92.
19. Zhao X, Yang J, Zhang X, Lu XA, Xiong M, Zhang J, et al. Efficacy and safety of CD28- or 4-1BB-based CD19 CAR-T cells in B cell acute lymphoblastic leukemia. Mol Ther Oncolytics 2020;18:272–81.
20. Schuster SJ, Maziarz RT, Rusch ES, Li J, Signorovitch JE, Romanov VV, et al. Grading and management of cytokine release syndrome in patients treated with tisagenlecleucel in the JULIET trial. Blood Adv 2020;4:1432–9.
21. Neelapu SS, Tummala S, Kebriaei P, Wierda W, Gutierrez C, Locke FL, et al. Chimeric antigen receptor T-cell therapy - assessment and management of toxicities. Nat Rev Clin Oncol 2018;15:47–62.
22. Maruoka H, Inoue D, Takiuchi Y, Nagano S, Arima H, Tabata S, et al. IP-10/CXCL10 and MIG/CXCL9 as novel markers for the diagnosis of lymphoma-associated hemophagocytic syndrome. Ann Hematol 2014;93:393–401.
23. Hallupp M, Stratling WH. A functional assay for enhancer-binding proteins. Nucleic Acids Res 1988;16:9870.
24. Lounder DT, Bin Q, de Min C, Jordan MB. Treatment of refractory hemophagocytic lymphohistiocytosis with emapalumab despite severe concurrent infections. Blood Adv 2019;3:47–50.
25. Norelli M, Camisa B, Barbiera G, Falcone L, Purevdorj A, Genua M, et al. Monocyte-derived IL-1 and IL-6 are differentially required for cytokine-release syndrome and neurotoxicity due to CAR T cells. Nat Med 2018;24:739–48.
26. Giavridis T, van der Stegen SJC, Eyquem J, Hamieh M, Piersigilli A, Sadelain M. CAR T cell-induced cytokine release syndrome is mediated by macrophages and abated by IL-1 blockade. Nat Med 2018;24:731–8.
27. Si S, Teachey DT. Spotlight on tocilizumab in the treatment of CAR-T-cell-induced cytokine release syndrome: clinical evidence to date. Ther Clin Risk Manag 2020;16:705–14.
28. Strati P, Ahmed S, Kebriaei P, Nastoupil LJ, Claussen CM, Watson G, et al. Clinical efficacy of anakinra to mitigate CAR T-cell therapy-associated toxicity in large B-cell lymphoma. Blood Adv 2020;4:3123–7.
29. Singh N, Hofmann TJ, Gershenson Z, Levine BL, Grupp SA, Teachey DT, et al. Monocyte lineage-derived IL-6 does not affect chimeric antigen receptor T-cell function. Cytotherapy 2017;19:867–80.
30. Gust J, Ponce R, Liles WC, Garden GA, Turtle CJ. Cytokines in CAR T cell-associated neurotoxicity. Front Immunol 2020;11:577027.
31. Nishimoto N, Terao K, Mima T, Nakahara H, Takagi N, Kakehi T. Mechanisms and pathologic significances in increase in serum interleukin-6 (IL-6) and soluble IL-6 receptor after administration of an anti-IL-6 receptor antibody, tocilizumab, in patients with rheumatoid arthritis and Castleman disease. Blood 2008;112:3959–64.
32. Bailey SR, Nelson MH, Majchrzak K, Bowers JS, Wyatt MM, Smith AS, et al. Human CD26(high) T cells elicit tumor immunity against multiple malignancies via enhanced migration and persistence. Nat Commun 2017;8:1961.
33. Nelson MH, Knochelmann HM, Bailey SR, Huff LW, Bowers JS, Majchrzak-Kuligowska K, et al. Identification of human CD4(+) T cell populations with distinct antitumor activity. Sci Adv 2020;6:eaba7443.
34. Singh N, Lee YG, Shestova O, Ravikumar P, Hayer KE, Hong SJ, et al. Impaired death receptor signaling in leukemia causes antigen-independent resistance by inducing CAR T-cell dysfunction. Cancer Discov 2020;10:552–67.
35. Li AM, Hucks GE, Dinofia AM, Seif EE, Teachey DT, Baniewicz D, et al. Checkpoint inhibitors augment CD19-directed chimeric antigen receptor (CAR) T cell therapy in relapsed B-cell acute lymphoblastic leukemia. Blood 2018;132:556.
36. Grosser R, Cherkassky L, Chintala N, Adusumilli PS. Combination immunotherapy with CAR T cells and checkpoint blockade for the treatment of solid tumors. Cancer Cell 2019;36:471–82.
37. Gardner RA, Ceppi F, Rivers J, Annesley C, Summers C, Taraseviciute A, et al. Preemptive mitigation of CD19 CAR T-cell cytokine release syndrome without attenuation of antileukemic efficacy. Blood 2019;134:2149–58.
38. Locke FL, Neelapu SS, Bartlett NL, Lekakis LJ, Jacobson CA, Braunschweig I, et al. Prophylactic tocilizumab after axicabtagene ciloleucel (axi-cel;KTE-C19) treatment for patients with reffractory, aggressive non-Hodgkin lymphoma (NHL). Blood 2017;130:1547.
39. Kambhampati S, Gray L, Fakhri B, Lo M, Vu K, Arora S, et al. Immune-related adverse events associated with checkpoint inhibition in the setting of CAR T cell therapy: a case series. Clin Lymphoma Myeloma Leuk 2020;20:e118–e23.
40. Ishii K, Pouzolles M, Chien CD, Erwin-Cohen RA, Kohler ME, Qin H, et al. Perforin-deficient CAR T cells recapitulate late-onset inflammatory toxicities observed in patients. J Clin Invest 2020;130:5425–43.
41. Valente G, Ozmen L, Novelli F, Geuna M, Palestro G, Forni G, et al. Distribution of interferon-gamma receptor in human tissues. Eur J Immunol 1992;22:2403–12.
42. Costa LJ, Mailankody S, Shaughnessy P, Hari P, Kaufman JL, Larson SM, et al. Anakinra (AKR) prophylaxis (ppx) in patients (pts) with relapsed/refractory multiple myeloma (RRMM) receiving orvacabtagene autoleucel (orva-cel). J Clin Oncol 39, 2021 (suppl 15; abstr 2537).
43. Sterner RM, Sakemura R, Cox MJ, Yang N, Khadka RH, Forsman CL, et al. GM-CSF inhibition reduces cytokine release syndrome and neuroinflammation but enhances CAR-T cell function in xenografts. Blood 2019;133:697–709.
44. Doench JG, Fusi N, Sullender M, Hegde M, Vaimberg EW, Donovan KF, et al. Optimized sgRNA design to maximize activity and minimize off-target effects of CRISPR-Cas9. Nat Biotechnol 2016;34:184–91.
45. Zhang M, Hutter G, Kahn SA, Azad TD, Gholamin S, Xu CY, et al. Anti-CD47 treatment stimulates phagocytosis of glioblastoma by M1 and M2 polarized macrophages and promotes M1 polarized macrophages in vivo. PLoS One 2016;11:e0153550.